

The Hoyle state and its relatives: The C12 continuum



Thomas Neff

**“Nuclear Structure & Reactions:
Experimental and Ab Initio Theoretical Perspectives”**

**TRIUMF, Vancouver, Canada
February 21, 2014**

Overview



Unitary Correlation Operator Method

Fermionic Molecular Dynamics

Cluster States in ^{12}C

- FMD and microscopic cluster model
- electron scattering data – form factors

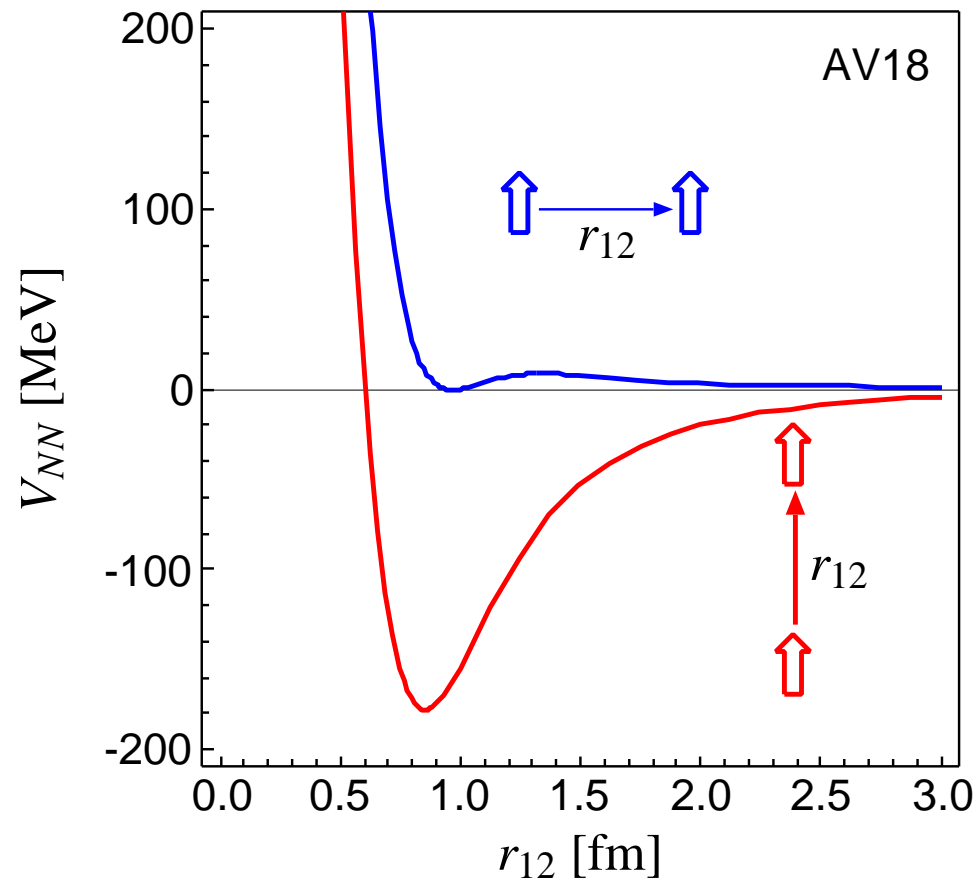
Resonances and Scattering States in ^{12}C

- include $^8\text{Be} + \alpha$ configurations
- *R*-matrix method

Nuclear Force

Argonne V18 (T=0)

spins aligned parallel or perpendicular to the relative distance vector



- strong repulsive core: nucleons can not get closer than ≈ 0.5 fm

➔ **central correlations**

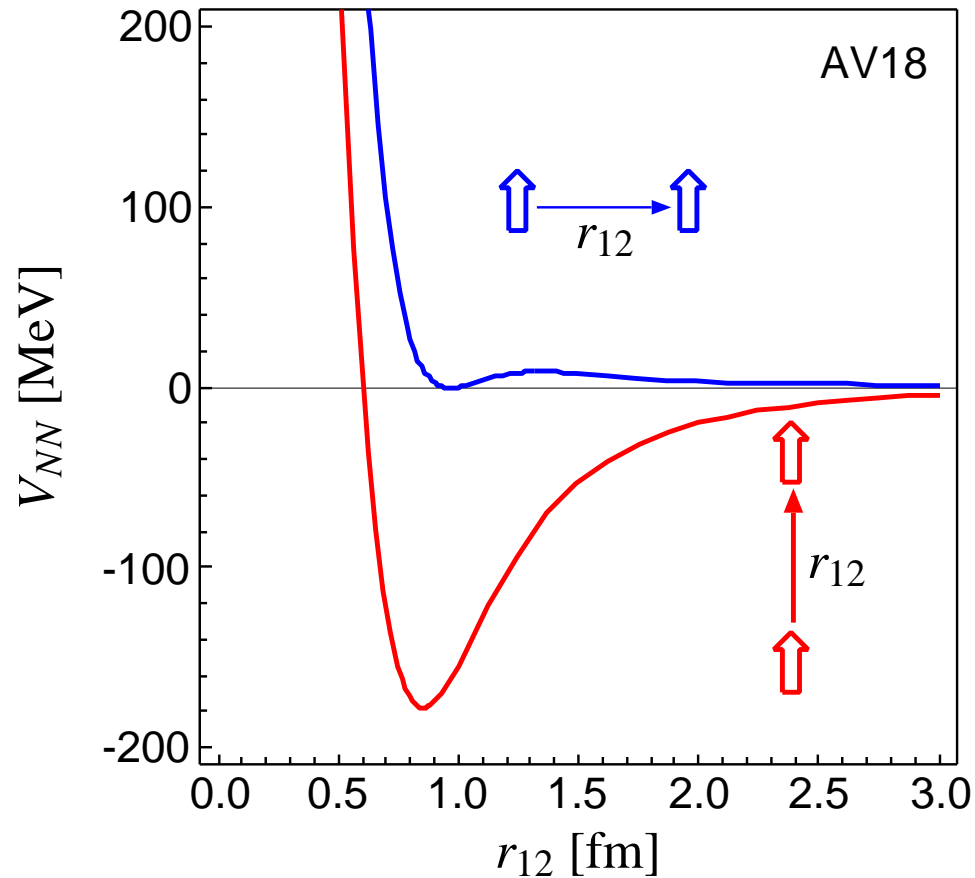
- strong dependence on the orientation of the spins due to the tensor force

➔ **tensor correlations**

Nuclear Force

Argonne V18 (T=0)

spins aligned parallel or perpendicular to the relative distance vector



- strong repulsive core: nucleons can not get closer than ≈ 0.5 fm

➔ **central correlations**

- strong dependence on the orientation of the spins due to the tensor force

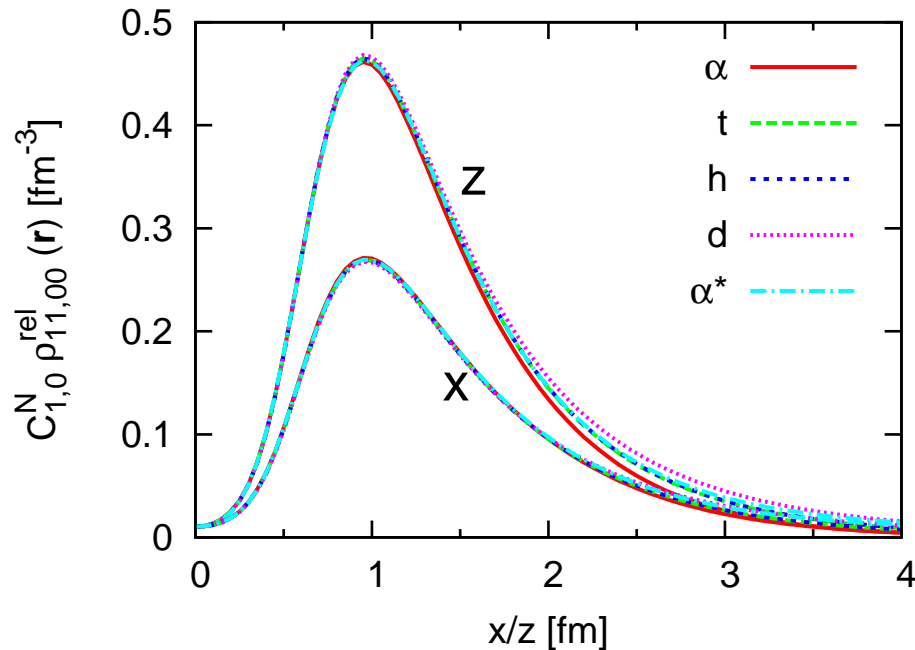
➔ **tensor correlations**

the nuclear force will induce **strong short-range correlations** in the nuclear wave function

- Universality of short-range correlations
- **Two-body densities in $A = 2, 3, 4$ Nuclei — AV8'**

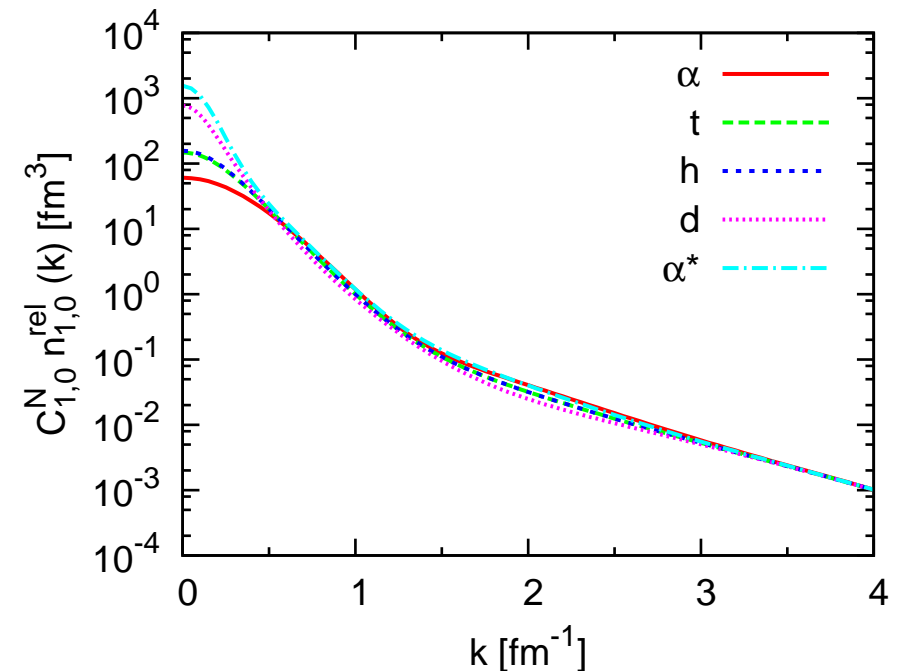
coordinate space

$S = 1, M_S = 1, T = 0$



momentum space

$S = 1, T = 0$



- normalize two-body density in coordinate space at $r=1.0$ fm
- normalized two-body densities in coordinate space are identical at short distances for all nuclei
- use the **same** normalization factor in momentum space – high momentum tails agree for all nuclei

Unitary Correlation Operator Method

Correlation Operator

- induce short-range (two-body) central and tensor correlations into the many-body state

$$\underline{C} = \underline{C}_\Omega \underline{C}_r = \exp\left[-i \sum_{i<j} \underline{g}_{\Omega,ij}\right] \exp\left[-i \sum_{i<j} \underline{g}_{r,ij}\right] \quad , \quad \underline{C}^\dagger \underline{C} = \underline{1}$$

- correlation operator should conserve the symmetries of the Hamiltonian and should be of finite-range, correlated interaction **phase shift equivalent** to bare interaction by construction

Correlated Operators

- correlated operators will have contributions in higher cluster orders

$$\underline{C}^\dagger \underline{O} \underline{C} = \hat{\underline{O}}^{[1]} + \hat{\underline{O}}^{[2]} + \hat{\underline{O}}^{[3]} + \dots$$

- two-body approximation: correlation range should be small compared to mean particle distance

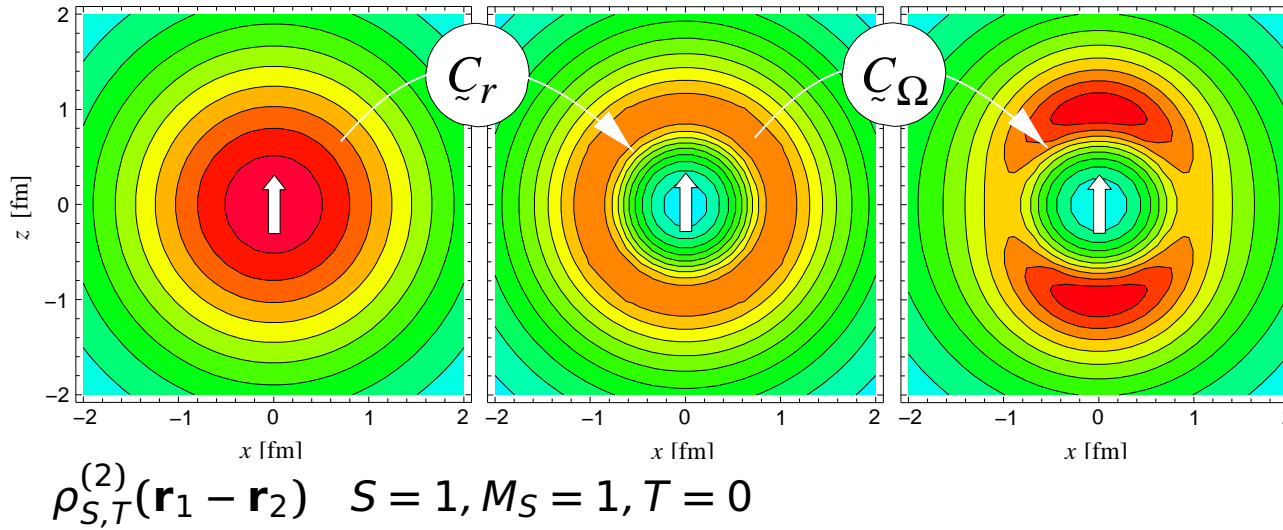
Correlated Interaction

$$\underline{C}^\dagger (\underline{T} + \underline{V}) \underline{C} = \underline{T} + \underline{V}_{\text{UCOM}} + \underline{V}_{\text{UCOM}}^{[3]} + \dots$$

Unitary Correlation Operator Method

Correlations and Energies

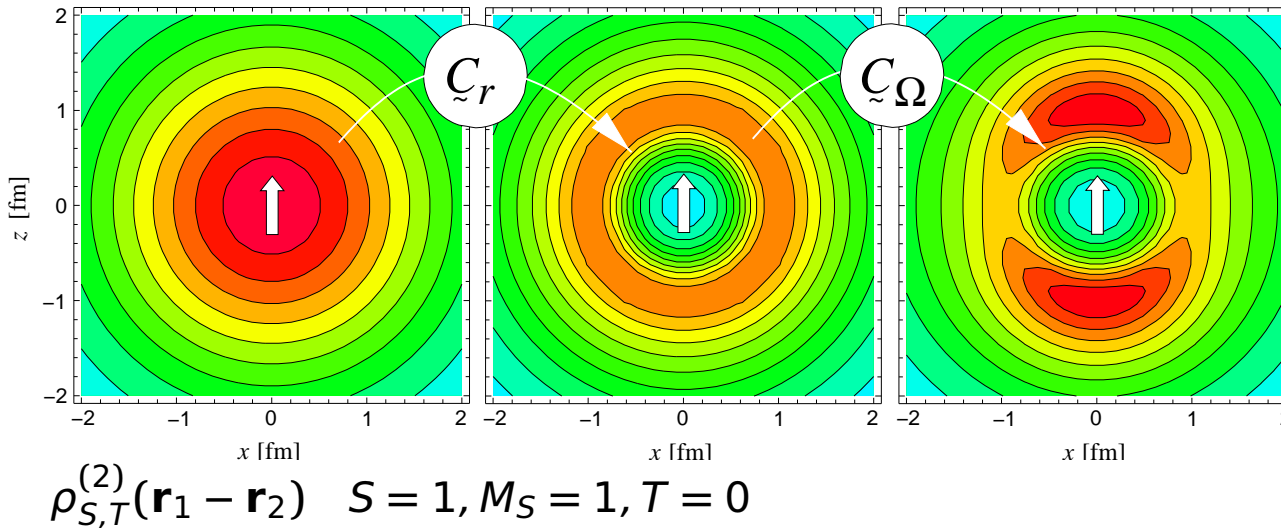
two-body densities



central correlator \tilde{C}_r
 shifts density out of
 the repulsive core
tensor correlator \tilde{C}_Ω
 aligns density with spin
 orientation

Unitary Correlation Operator Method Correlations and Energies

two-body densities

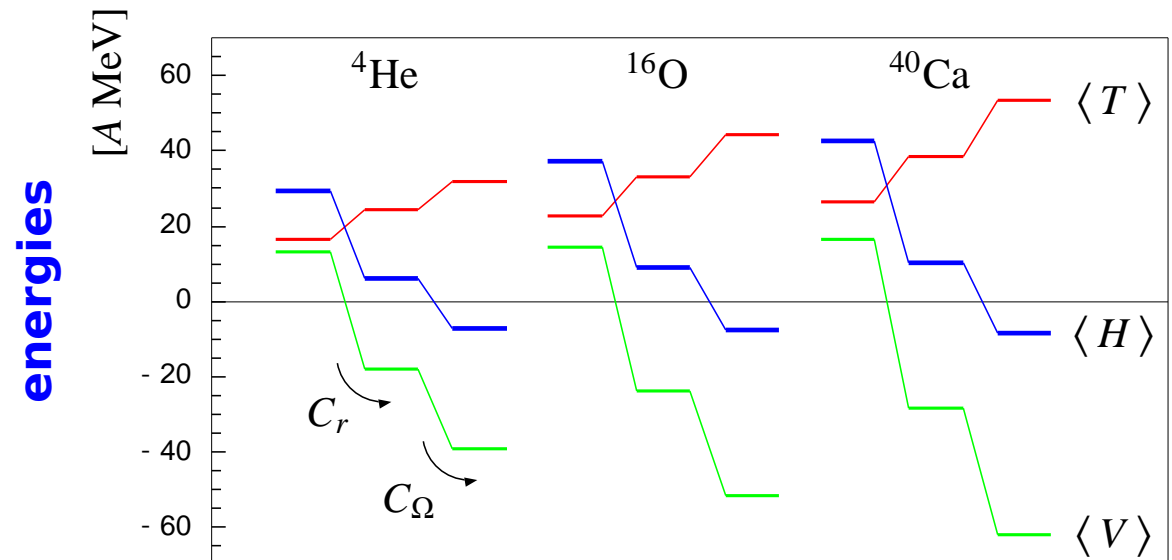


central correlator \tilde{C}_r
shifts density out of
the repulsive core

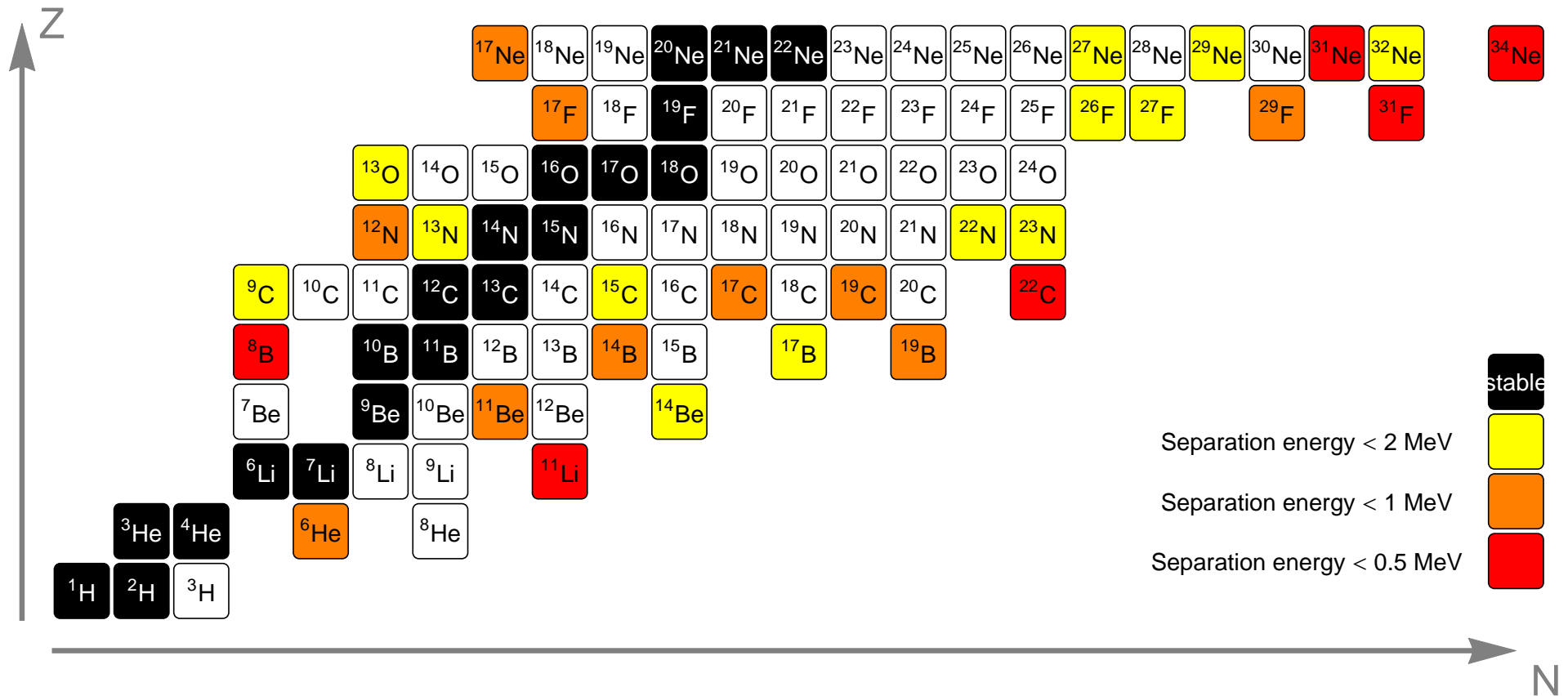
tensor correlator \tilde{C}_Ω
aligns density with spin
orientation

both central
and tensor
correlations are
essential for
binding

$0\hbar\omega$ Harmonic Oscillator



Exotica: Special Challenges



- ➔ states close to one-nucleon, two-nucleon or cluster thresholds can have well developed **halo** or **cluster** structure
- ➔ these are hard to tackle in the harmonic oscillator basis

Fermionic

Slater determinant

$$|Q\rangle = \mathcal{A}\left(|q_1\rangle \otimes \cdots \otimes |q_A\rangle\right)$$

- antisymmetrized A -body state

Fermionic

Slater determinant

$$|Q\rangle = \mathcal{A}\left(|q_1\rangle \otimes \cdots \otimes |q_A\rangle\right)$$

- antisymmetrized A -body state

Molecular

single-particle states

$$\langle \mathbf{x} | q \rangle = \sum_i c_i \exp\left\{-\frac{(\mathbf{x} - \mathbf{b}_i)^2}{2a_i}\right\} \otimes |\chi_i^\uparrow, \chi_i^\downarrow\rangle \otimes |\xi\rangle$$

- Gaussian wave-packets in phase-space (complex parameter \mathbf{b}_i encodes mean position and mean momentum), spin is free, isospin is fixed
- width a_i is an independent variational parameter for each wave packet
- use one or two wave packets for each single particle state

Fermionic

Slater determinant

$$|Q\rangle = \mathcal{A}\left(|q_1\rangle \otimes \cdots \otimes |q_A\rangle\right)$$

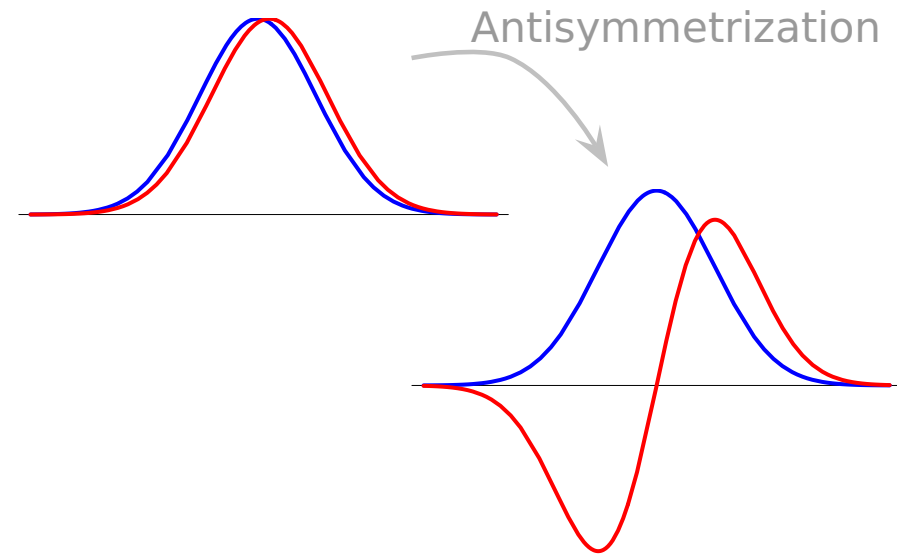
- antisymmetrized A-body state

Molecular

single-particle states

$$\langle \mathbf{x} | q \rangle = \sum_i c_i \exp\left\{-\frac{(\mathbf{x} - \mathbf{b}_i)^2}{2a_i}\right\} \otimes |\chi_i^\uparrow, \chi_i^\downarrow\rangle \otimes |\xi\rangle$$

- Gaussian wave-packets in phase-space (complex parameter \mathbf{b}_i encodes mean position and mean momentum), spin is free, isospin is fixed
- width a_i is an independent variational parameter for each wave packet
- use one or two wave packets for each single particle state



Fermionic

Slater determinant

$$|Q\rangle = \mathcal{A}\left(|q_1\rangle \otimes \cdots \otimes |q_A\rangle\right)$$

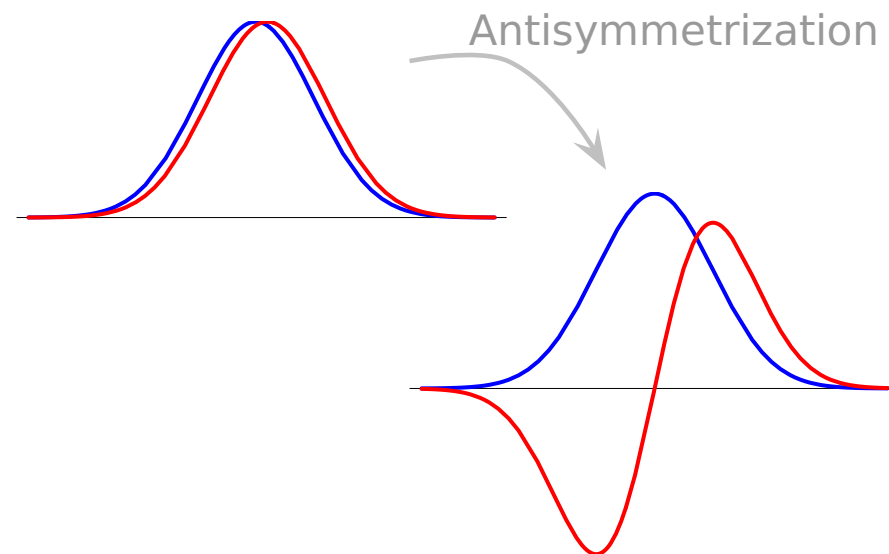
- antisymmetrized A-body state

Molecular

single-particle states

$$\langle \mathbf{x} | q \rangle = \sum_i c_i \exp\left\{-\frac{(\mathbf{x} - \mathbf{b}_i)^2}{2a_i}\right\} \otimes |\chi_i^\uparrow, \chi_i^\downarrow\rangle \otimes |\xi\rangle$$

- Gaussian wave-packets in phase-space (complex parameter \mathbf{b}_i encodes mean position and mean momentum), spin is free, isospin is fixed
- width a_i is an independent variational parameter for each wave packet
- use one or two wave packets for each single particle state



see also
**Antisymmetrized
 Molecular Dynamics**
 Horiuchi, Kanada-En'yo,
 Kimura, ...

Operator Representation of V_{UCOM}

$$\tilde{\zeta}^\dagger (\tilde{T} + \tilde{V}) \tilde{\zeta} = \tilde{T}$$

$$+ \sum_{ST} \hat{V}_c^{ST}(r) + \frac{1}{2} (p_r^2 \hat{V}_{p^2}^{ST}(r) + \hat{V}_{p^2}^{ST}(r) p_r^2) + \hat{V}_{l^2}^{ST}(r) \mathbf{l}^2$$

one-body kinetic energy

central potentials

$$+ \sum_T \hat{V}_{ls}^T(r) \mathbf{l} \cdot \mathbf{s} + \hat{V}_{l^2ls}^T(r) \mathbf{l}^2 \mathbf{l} \cdot \mathbf{s}$$

spin-orbit potentials

$$+ \sum_T \hat{V}_t^T(r) \mathcal{S}_{12}(\mathbf{r}, \mathbf{r}) + \hat{V}_{trp_\Omega}^T(r) p_r \mathcal{S}_{12}(\mathbf{r}, \mathbf{p}_\Omega) + \hat{V}_{tll}^T(r) \mathcal{S}_{12}(\mathbf{l}, \mathbf{l}) +$$

$$\hat{V}_{tp_\Omega p_\Omega}^T(r) \mathcal{S}_{12}(\mathbf{p}_\Omega, \mathbf{p}_\Omega) + \hat{V}_{l^2tp_\Omega p_\Omega}^T(r) \mathbf{l}^2 \mathcal{S}_{12}(\mathbf{p}_\Omega, \mathbf{p}_\Omega)$$

tensor potentials

bulk of tensor force mapped onto central part
of correlated interaction
tensor correlations also change the spin-orbit
part of the interaction

Projection After Variation (PAV)

- mean-field may break symmetries of Hamiltonian
- restore inversion, translational and rotational symmetry by projection on parity, linear and angular momentum

$$\tilde{P}^\pi = \frac{1}{2}(1 + \pi\Pi)$$

$$\tilde{P}_{MK}^J = \frac{2J+1}{8\pi^2} \int d^3\Omega D_{MK}^{J*}(\Omega) R(\Omega)$$

$$\tilde{P}^{\mathbf{P}} = \frac{1}{(2\pi)^3} \int d^3\mathbf{X} \exp\{-i(\tilde{\mathbf{P}} - \mathbf{P}) \cdot \mathbf{X}\}$$

Projection After Variation (PAV)

- mean-field may break symmetries of Hamiltonian
- restore inversion, translational and rotational symmetry by projection on parity, linear and angular momentum

$$\tilde{P}^{\pi} = \frac{1}{2}(1 + \pi\Pi)$$

$$\tilde{P}_{MK}^J = \frac{2J+1}{8\pi^2} \int d^3\Omega D_{MK}^{J*}(\Omega) \tilde{R}(\Omega)$$

Variation After Projection (VAP)

- effect of projection can be large
- **Variation after Angular Momentum and Parity Projection** (VAP) for light nuclei
- combine VAP with **constraints** on **radius**, **dipole** moment, **quadrupole** moment, ... to generate additional configurations

$$\tilde{P}^{\mathbf{P}} = \frac{1}{(2\pi)^3} \int d^3\mathbf{X} \exp\{-i(\tilde{\mathbf{P}} - \mathbf{P}) \cdot \mathbf{X}\}$$

PAV, VAP and Multiconfiguration

Projection After Variation (PAV)

- mean-field may break symmetries of Hamiltonian
- restore inversion, translational and rotational symmetry by projection on parity, linear and angular momentum

$$\tilde{P}^\pi = \frac{1}{2}(1 + \pi\Pi)$$

$$\tilde{P}_{MK}^J = \frac{2J+1}{8\pi^2} \int d^3\Omega D_{MK}^{J*}(\Omega) \tilde{R}(\Omega)$$

Variation After Projection (VAP)

- effect of projection can be large
- **Variation after Angular Momentum and Parity Projection** (VAP) for light nuclei
- combine VAP with **constraints** on **radius**, **dipole** moment, **quadrupole** moment, ... to generate additional configurations

$$\tilde{P}^{\mathbf{P}} = \frac{1}{(2\pi)^3} \int d^3\mathbf{X} \exp\{-i(\tilde{\mathbf{P}} - \mathbf{P}) \cdot \mathbf{X}\}$$

Multiconfiguration Calculations

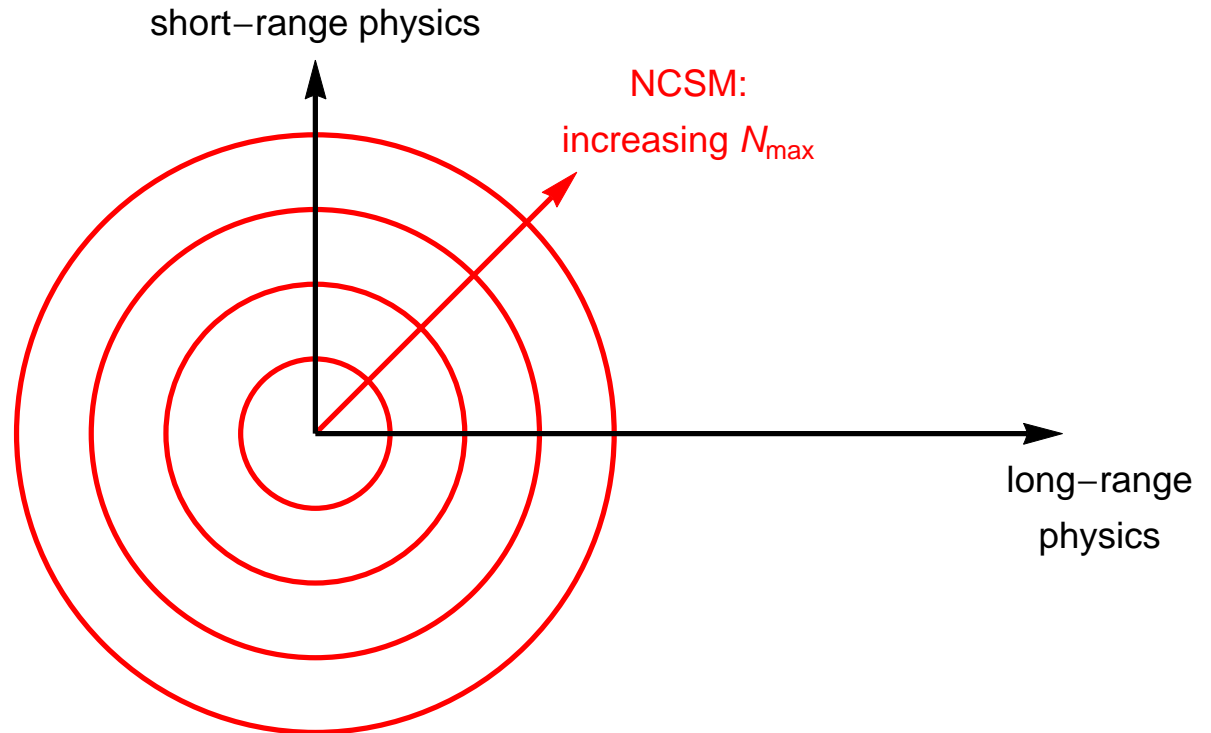
- **diagonalize** Hamiltonian in a set of projected intrinsic states

$$\left\{ |Q^{(a)}\rangle, \quad a = 1, \dots, N \right\}$$

$$\sum_{K'b} \langle Q^{(a)} | \tilde{H} \tilde{P}_{KK'}^{J\pi} \tilde{P}^{\mathbf{P}=0} | Q^{(b)} \rangle \cdot c_{K'b}^\alpha = E^{J\pi\alpha} \sum_{K'b} \langle Q^{(a)} | \tilde{P}_{KK'}^{J\pi} \tilde{P}^{\mathbf{P}=0} | Q^{(b)} \rangle \cdot c_{K'b}^\alpha$$

- FMD

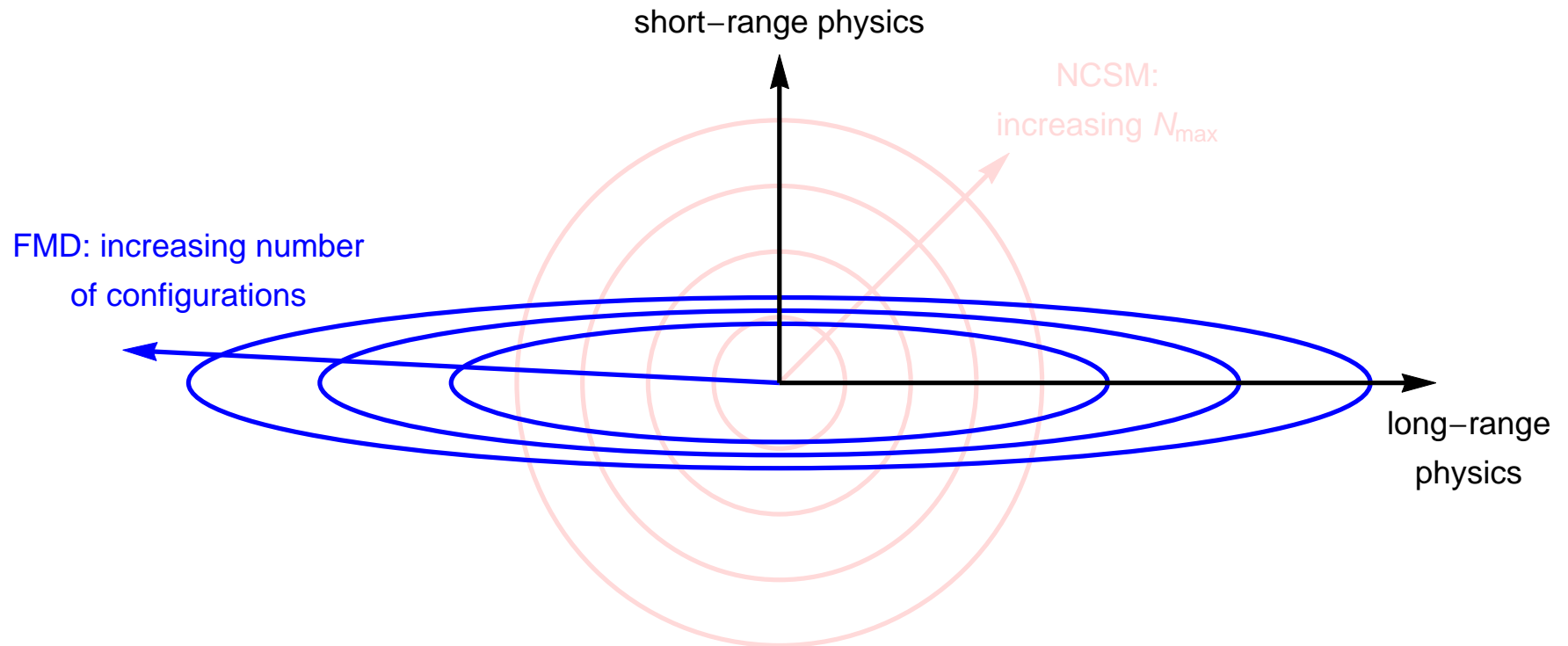
- **FMD vs NCSM model spaces**



- NCSM allows good description of short-range physics, but long-range behavior suffers from harmonic oscillator asymptotics

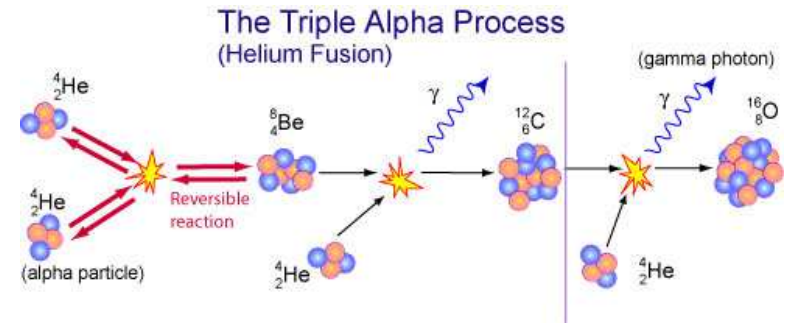
• FMD

• FMD vs NCSM model spaces



- NCSM allows good description of short-range physics, but long-range behavior suffers from harmonic oscillator asymptotics
- FMD allows to describe long-range physics by superposition of localized cluster configurations, but limited in description of short-range physics

Cluster States in ^{12}C

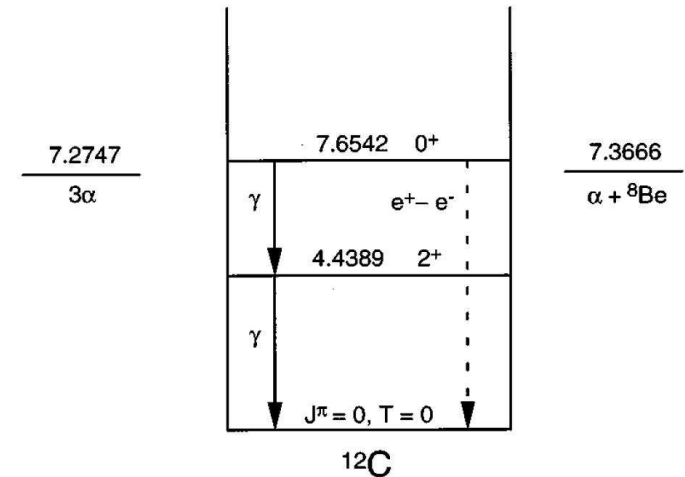


Astrophysical Motivation

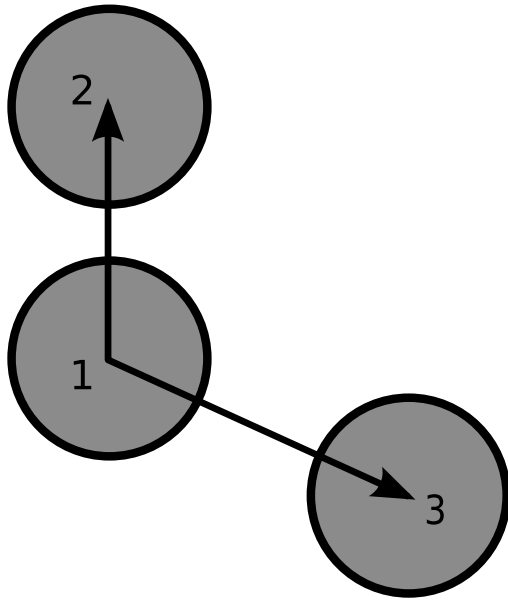
- Helium burning: triple alpha-reaction

Structure

- Is the Hoyle state a pure α -cluster state ?
- Other excited 0^+ and 2^+ states
- ➔ Compare FMD results to microscopic α -cluster model
- ➔ Intrinsic structure from two-body densities
- ➔ Analyze wave functions in harmonic oscillator basis



Microscopic α -Cluster Model



$$R_{12} = (2, 4, \dots, 10) \text{ fm}$$

$$R_{13} = (2, 4, \dots, 10) \text{ fm}$$

$$\cos(\vartheta) = (1.0, 0.8, \dots, -1.0)$$

altogether 165 configurations

Basis States

- describe Hoyle State as a system of 3 ^4He nuclei

$$|\psi_{3\alpha}(\mathbf{R}_1, \mathbf{R}_2, \mathbf{R}_3); JMK\pi\rangle = P_{MK}^J P^\pi \mathcal{A} \{ |\psi_\alpha(\mathbf{R}_1)\rangle \otimes |\psi_\alpha(\mathbf{R}_2)\rangle \otimes |\psi_\alpha(\mathbf{R}_3)\rangle \}$$

Volkov Interaction

- simple central interaction
- parameters adjusted to give reasonable α binding energy and radius, $\alpha - \alpha$ scattering data, adjusted to reproduce ^{12}C ground state energy

✗ only reasonable for ^4He , ^8Be and ^{12}C nuclei

'BEC' wave functions

- interpretation of the Hoyle state as a Bose-Einstein Condensate of α -particles by Funaki, Tohsaki, Horiuchi, Schuck, Röpke
- same interaction and α -cluster parameters used

Cluster States in ^{12}C

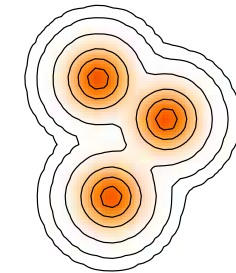
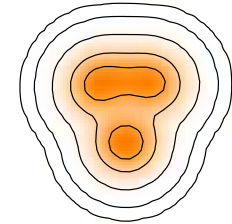
FMD

Basis States

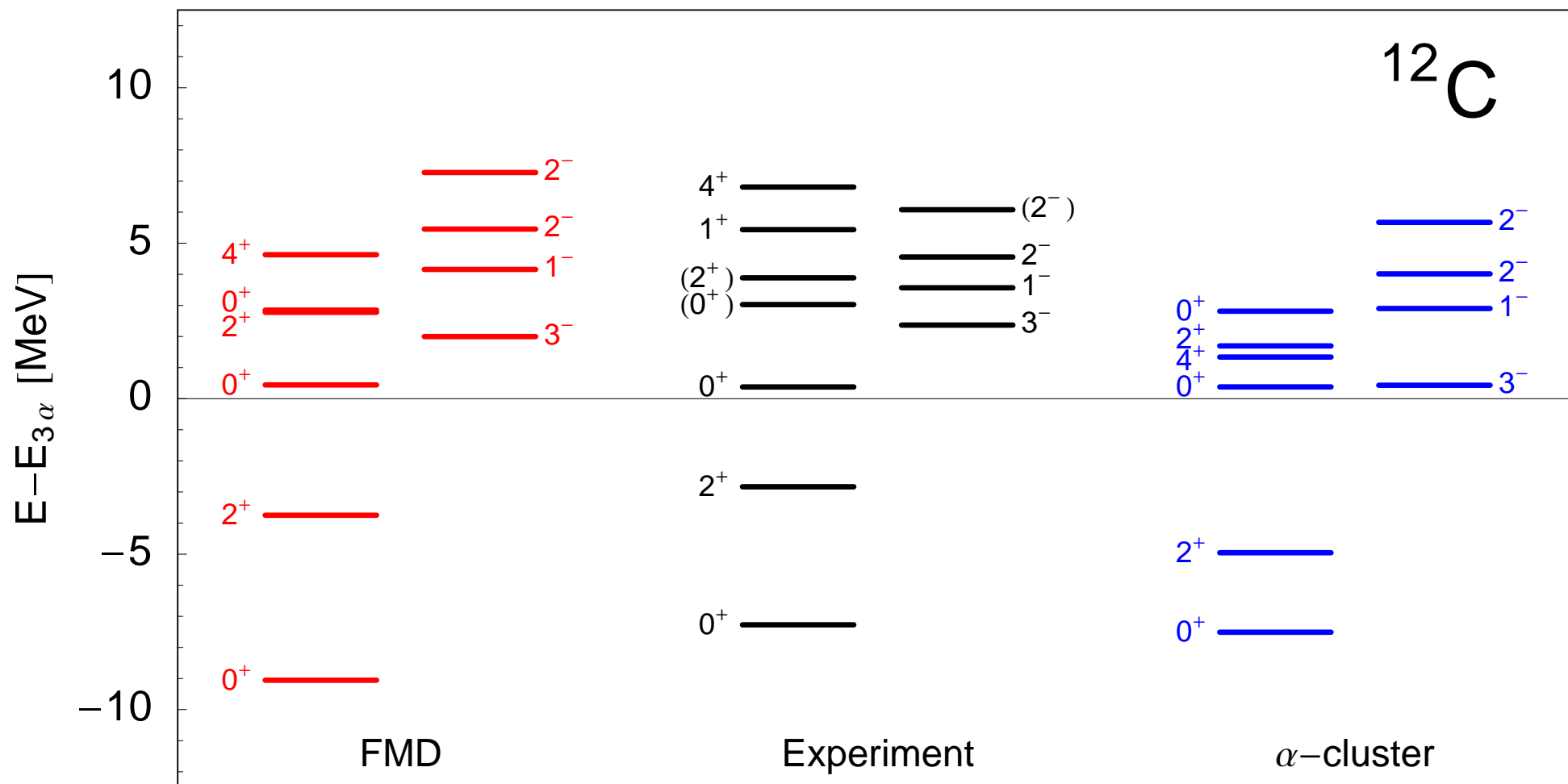
- 20 FMD states obtained in Variation after Projection on 0^+ and 2^+ with constraints on the radius
- 42 FMD states obtained in Variation after Projection on parity with constraints on radius and quadrupole deformation
- 165 α -cluster configurations
- ➔ projected on angular momentum and linear momentum

Interaction

- UCOM interaction ($I_9=0.30 \text{ fm}^3$ with phenomenological two-body correction term (momentum-dependent central and spin-orbit) fitted to doubly-magic nuclei
- not tuned for α - α scattering or ^{12}C properties



Cluster States in ^{12}C Comparison



Cluster States in ^{12}C Comparison

| | Exp ¹ | Exp ² | FMD | α -cluster | 'BEC' ³ |
|----------------------------------|------------------|------------------|--------|-------------------|--------------------|
| $E(0_1^+)$ | -92.16 | | -92.64 | -89.56 | -89.52 |
| $E^*(2_1^+)$ | 4.44 | | 5.31 | 2.56 | 2.81 |
| $E(3\alpha)$ | -84.89 | | -83.59 | -82.05 | -82.05 |
| $E(0_2^+) - E(3\alpha)$ | 0.38 | | 0.43 | 0.38 | 0.26 |
| $E(0_3^+) - E(3\alpha)$ | (3.0) | 2.7(3) | 2.84 | 2.81 | |
| $E(2_2^+) - E(3\alpha)$ | (3.89) | 2.76(11) | 2.77 | 1.70 | |
| $r_{\text{charge}}(0_1^+)$ | 2.47(2) | | 2.53 | 2.54 | |
| $r(0_1^+)$ | | | 2.39 | 2.40 | 2.40 |
| $r(0_2^+)$ | | | 3.38 | 3.71 | 3.83 |
| $r(0_3^+)$ | | | 4.62 | 4.75 | |
| $r(2_1^+)$ | | | 2.50 | 2.37 | 2.38 |
| $r(2_2^+)$ | | | 4.43 | 4.02 | |
| $M(E0, 0_1^+ \rightarrow 0_2^+)$ | 5.4(2) | | 6.53 | 6.52 | 6.45 |
| $B(E2, 2_1^+ \rightarrow 0_1^+)$ | 7.6(4) | | 8.69 | 9.16 | |
| $B(E2, 2_1^+ \rightarrow 0_2^+)$ | 2.6(4) | | 3.83 | 0.84 | |
| $B(E2, 2_2^+ \rightarrow 0_1^+)$ | | 0.73(13) | 0.46 | 1.99 | |

experimental situation
for 0^+ and 2^+ states
above threshold still
not completely settled

¹ Ajzenberg-Selove, Nuc. Phys. **A506**, 1 (1990)

² Itoh et al., Nuc. Phys. **A738**, 268 (2004), Zimmermann et al., Phys. Rev. Lett. **110**, 152502 (2013)

³ Funaki et al., Phys. Rev. C **67**, 051306(R) (2003)

Cluster States in ^{12}C Comparison

| | Exp ¹ | Exp ² | FMD | α -cluster | 'BEC' ³ |
|----------------------------------|------------------|------------------|--------|-------------------|--------------------|
| $E(0_1^+)$ | -92.16 | | -92.64 | -89.56 | -89.52 |
| $E^*(2_1^+)$ | 4.44 | | 5.31 | 2.56 | 2.81 |
| $E(3\alpha)$ | -84.89 | | -83.59 | -82.05 | -82.05 |
| $E(0_2^+) - E(3\alpha)$ | 0.38 | | 0.43 | 0.38 | 0.26 |
| $E(0_3^+) - E(3\alpha)$ | (3.0) | 2.7(3) | 2.84 | 2.81 | |
| $E(2_2^+) - E(3\alpha)$ | (3.89) | 2.76(11) | 2.77 | 1.70 | |
| $r_{\text{charge}}(0_1^+)$ | 2.47(2) | | 2.53 | 2.54 | |
| $r(0_1^+)$ | | | 2.39 | 2.40 | 2.40 |
| $r(0_2^+)$ | | | 3.38 | 3.71 | 3.83 |
| $r(0_3^+)$ | | | 4.62 | 4.75 | |
| $r(2_1^+)$ | | | 2.50 | 2.37 | 2.38 |
| $r(2_2^+)$ | | | 4.43 | 4.02 | |
| $M(E0, 0_1^+ \rightarrow 0_2^+)$ | 5.4(2) | | 6.53 | 6.52 | 6.45 |
| $B(E2, 2_1^+ \rightarrow 0_1^+)$ | 7.6(4) | | 8.69 | 9.16 | |
| $B(E2, 2_1^+ \rightarrow 0_2^+)$ | 2.6(4) | | 3.83 | 0.84 | |
| $B(E2, 2_2^+ \rightarrow 0_1^+)$ | | 0.73(13) | 0.46 | 1.99 | |

experimental situation
for 0^+ and 2^+ states
above threshold still
not completely settled

calculated in bound
state approximation

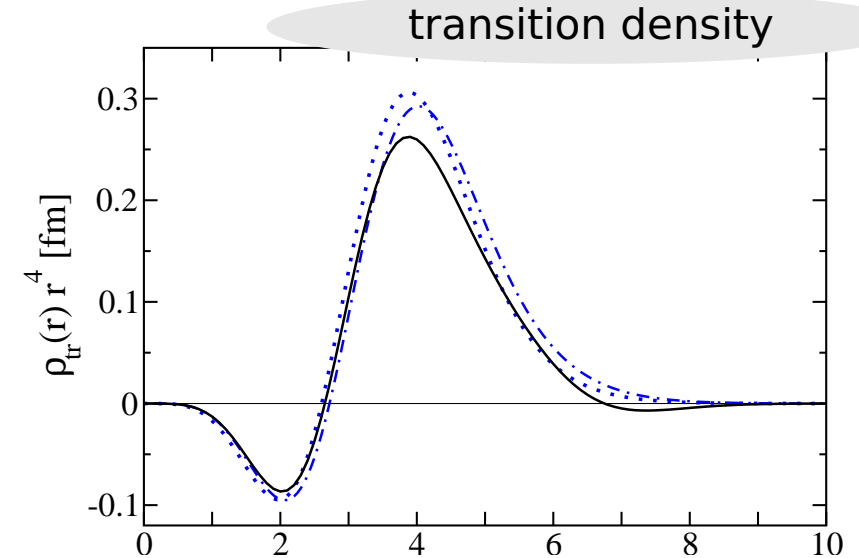
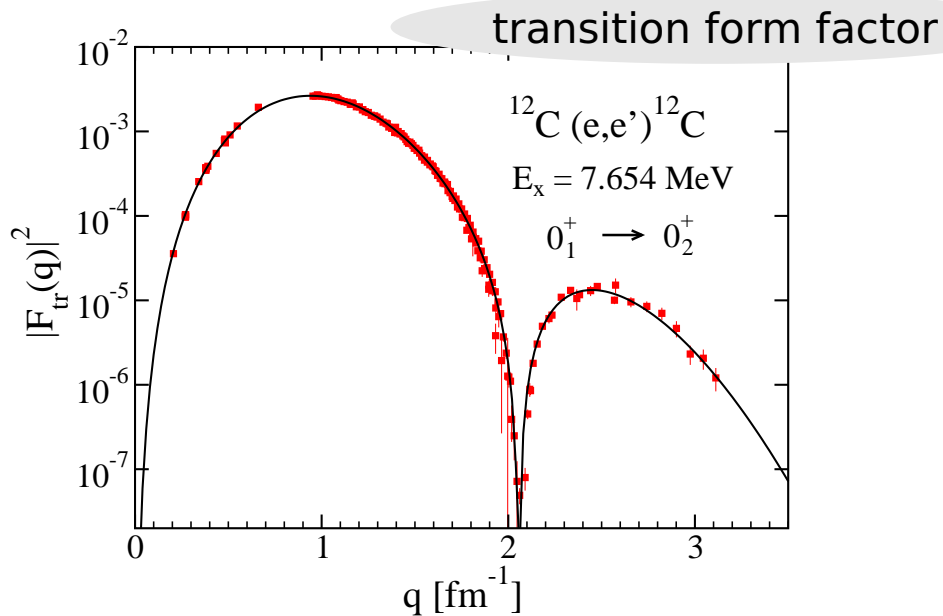
¹ Ajzenberg-Selove, Nuc. Phys. **A506**, 1 (1990)

² Itoh et al., Nuc. Phys. **A738**, 268 (2004), Zimmermann et al., Phys. Rev. Lett. **110**, 152502 (2013)

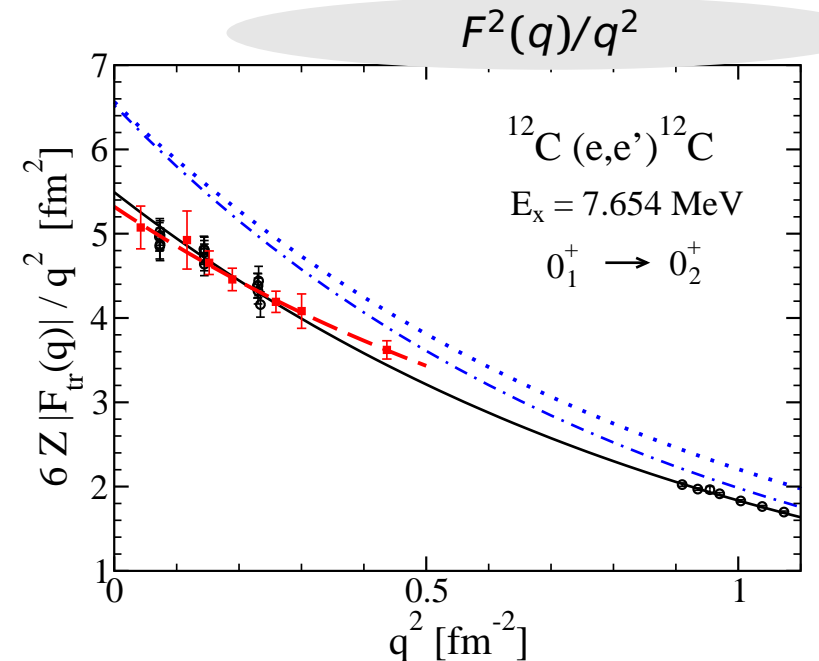
³ Funaki et al., Phys. Rev. C **67**, 051306(R) (2003)

Cluster States in ^{12}C

Monopole Matrix Element revisited

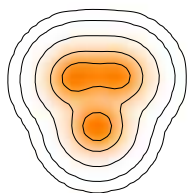


- $M(E0)$ determines the pair decay width
- model-independent self-consistent determination of transition form-factor/density in DWBA
- data at high momentum transfer necessary to constrain matrix element
 $M(E0) = 5.47 \pm 0.09 e^2 \text{fm}^2$

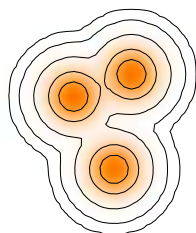


Cluster States in ^{12}C Important Configurations

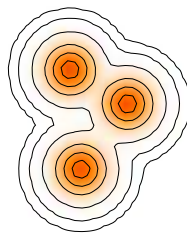
- Calculate the overlap with FMD basis states to find the most important contributions to the Hoyle state



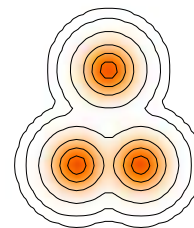
$$\begin{aligned} |\langle \cdot | 0_1^+ \rangle| &= 0.94 \\ |\langle \cdot | 2_1^+ \rangle| &= 0.93 \end{aligned}$$



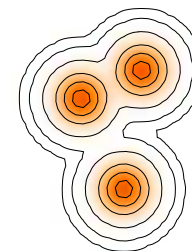
$$|\langle \cdot | 0_2^+ \rangle| = 0.72$$



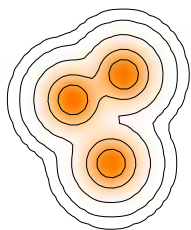
$$|\langle \cdot | 0_2^+ \rangle| = 0.71$$



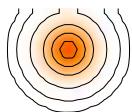
$$|\langle \cdot | 0_2^+ \rangle| = 0.61$$



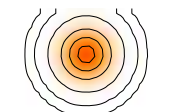
$$|\langle \cdot | 0_2^+ \rangle| = 0.61$$



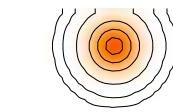
$$|\langle \cdot | 3_1^- \rangle| = 0.83$$



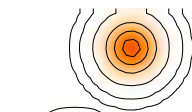
$$|\langle \cdot | 0_3^+ \rangle| = 0.50$$



$$|\langle \cdot | 0_3^+ \rangle| = 0.49$$



$$|\langle \cdot | 0_3^+ \rangle| = 0.44$$

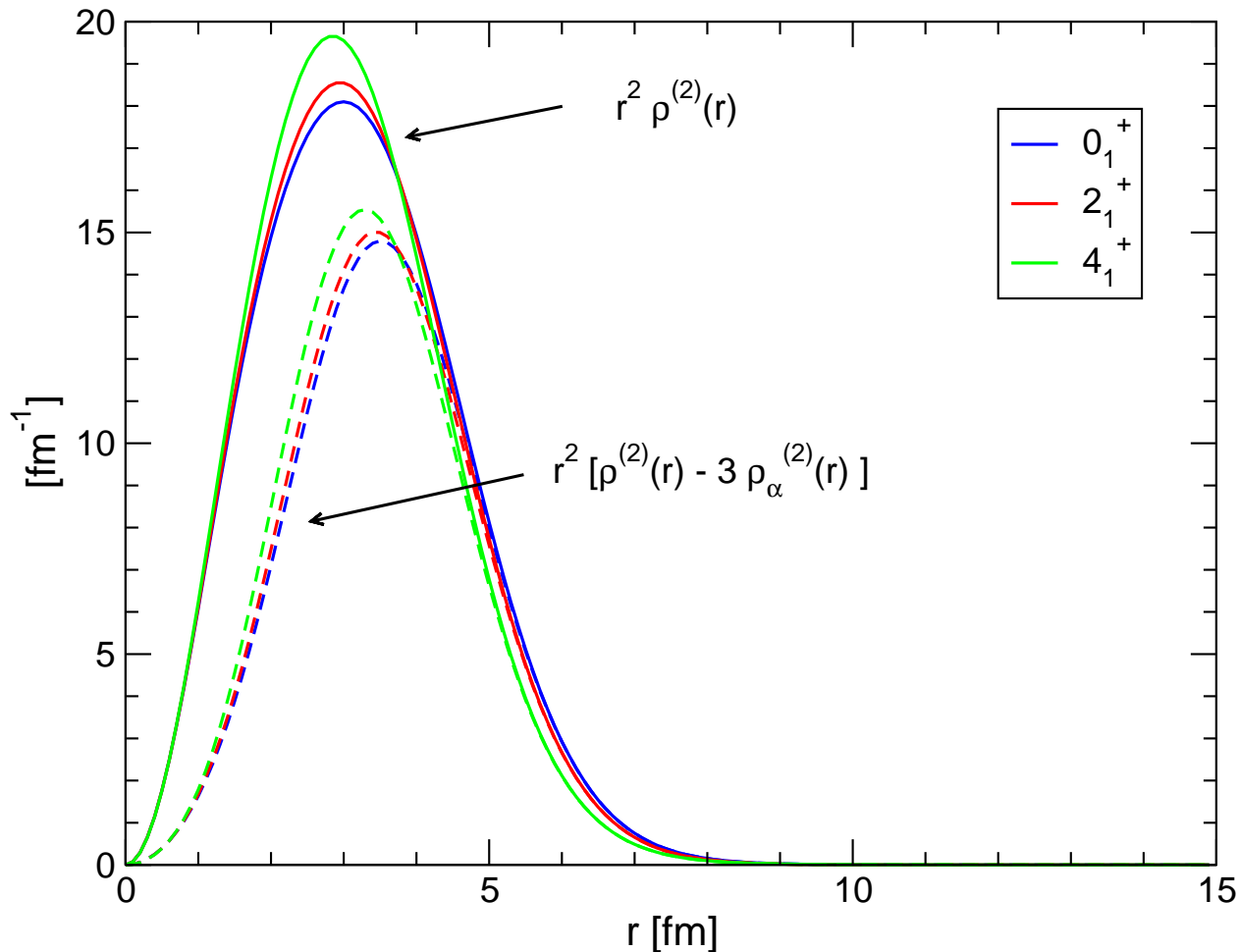


$$|\langle \cdot | 0_3^+ \rangle| = 0.41$$

FMD basis states are not orthogonal!

0_2^+ and 0_3^+ states have no rigid intrinsic structure

ground state band



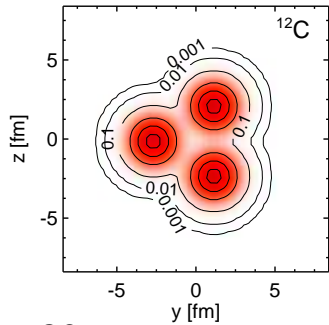
Cluster Model

$$\rho^{(2)}(r) = \langle \Psi | \sum_{i < j} \delta(\mathbf{r} - \mathbf{r}_{ij}) | \Psi \rangle$$

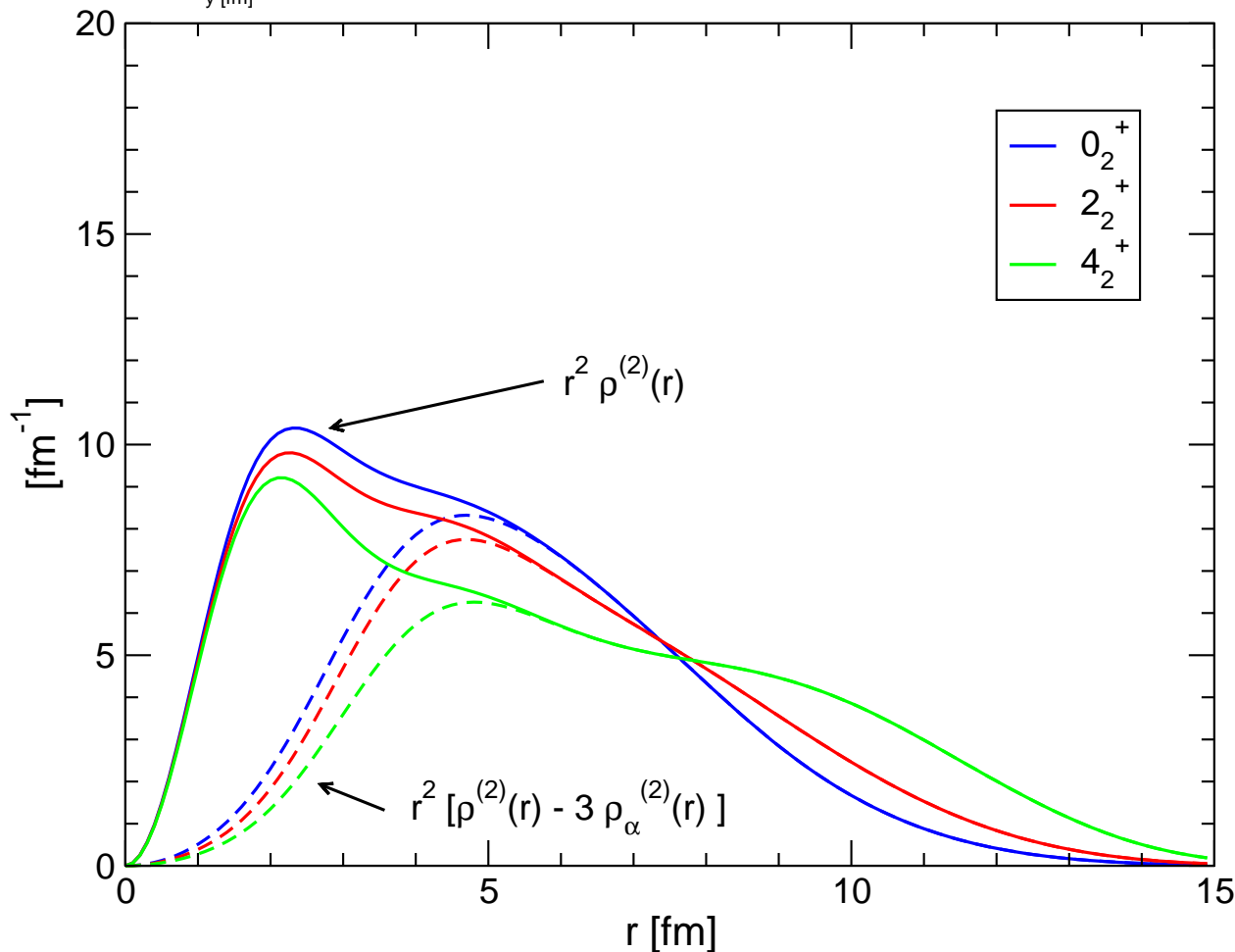
- subtract contributions from α 's to extract " α - α " correlations
- (subtracted) two-body density peaks at 3.5 fm
- ➔ consistent with **compact triangular structure**

Cluster States in ^{12}C

Two-body Densities and Intrinsic Structure



Hoyle state "band"



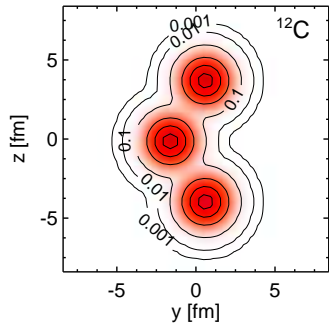
Cluster Model

$$\rho^{(2)}(r) = \langle \Psi | \sum_{i < j} \delta(\mathbf{r} - \mathbf{r}_{ij}) | \Psi \rangle$$

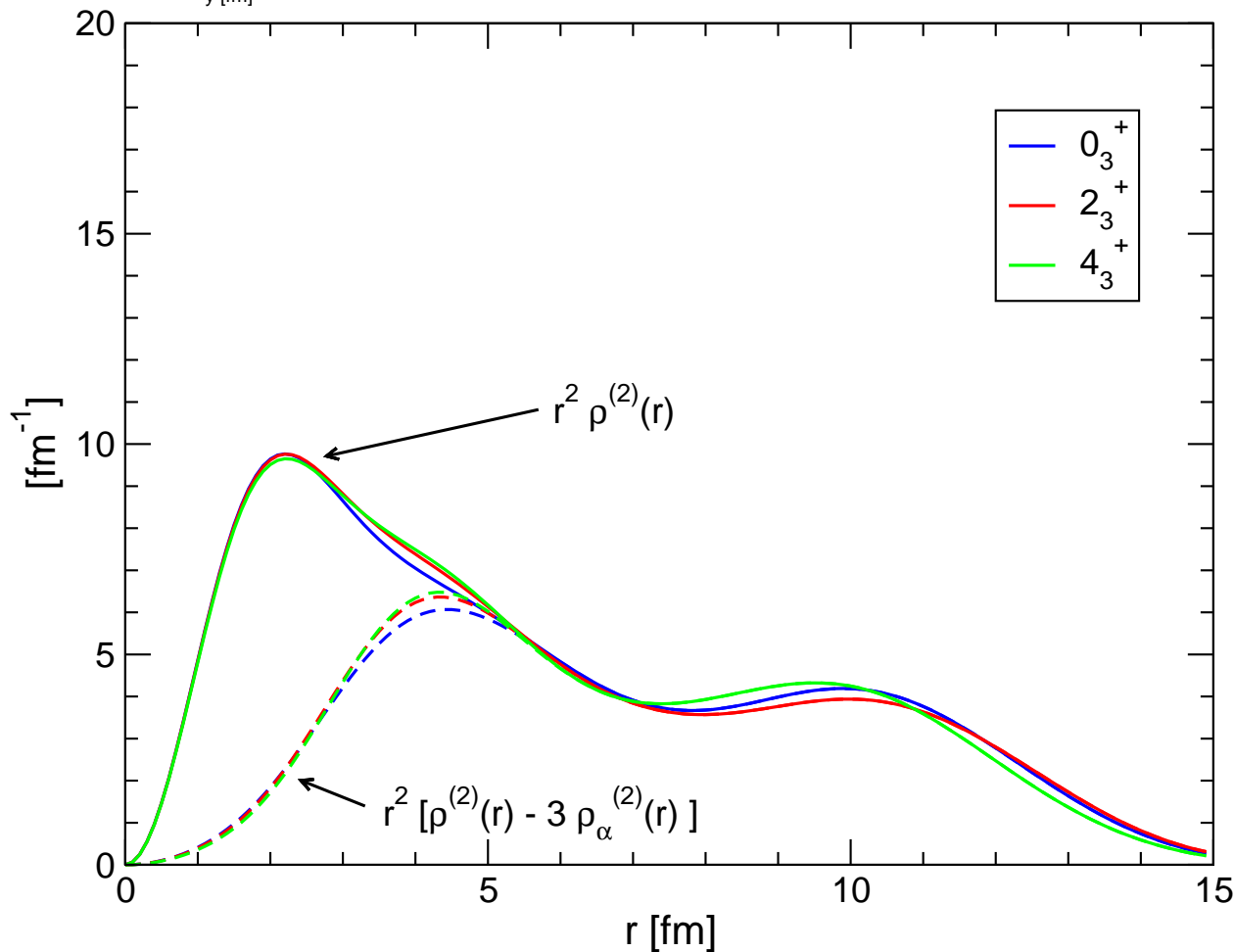
- subtract contributions from α 's to extract " α - α correlations"
- Hoyle state two-body density peaks at 5 fm, extended tail
- ➔ consistent with **triangular structure**
- tail in 2_2^+ and 4_2^+ states more pronounced
- ➔ admixture of open triangle configurations

Cluster States in ^{12}C

Two-body Densities and Intrinsic Structure



third 0^+ state band



Cluster Model

$$\rho^{(2)}(r) = \langle \Psi | \sum_{i < j} \delta(\mathbf{r} - \mathbf{r}_{ij}) | \Psi \rangle$$

- subtract contributions from α 's to extract " α - α " correlations
- two-body density peaks at 4.5 fm and 10 fm
- ➔ consistent with **open triangle/chain configuration**

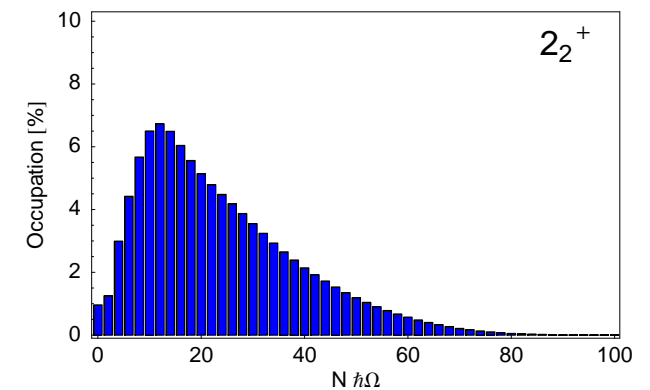
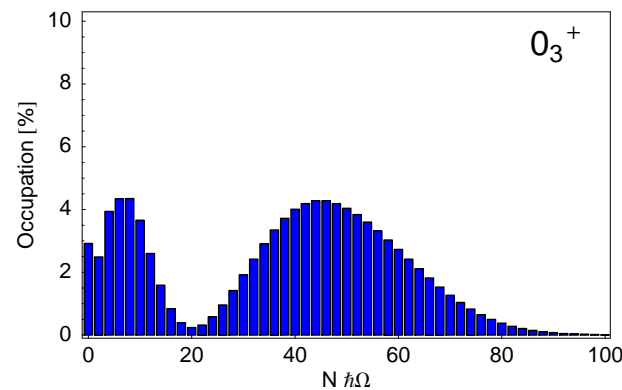
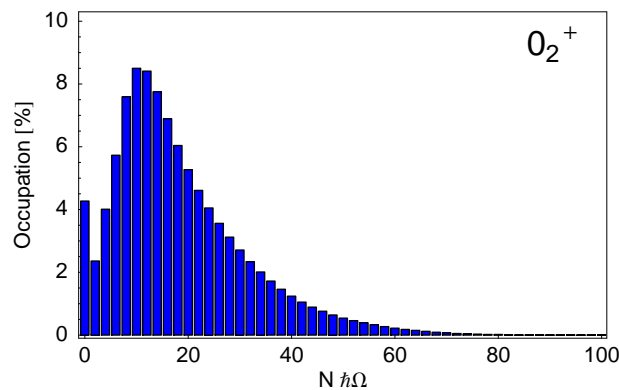
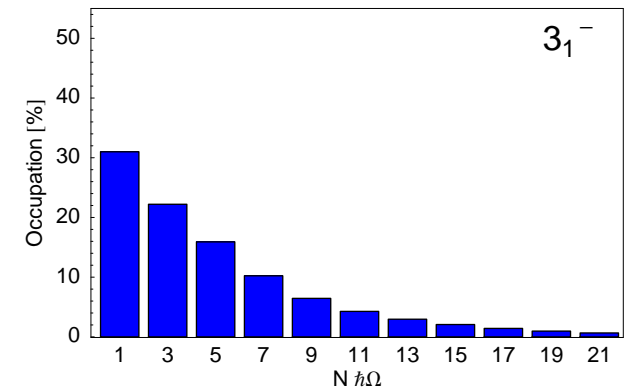
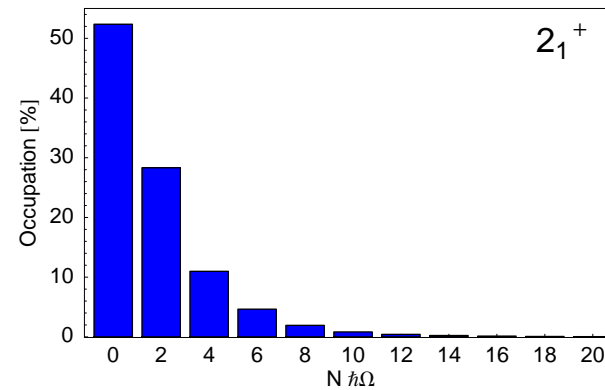
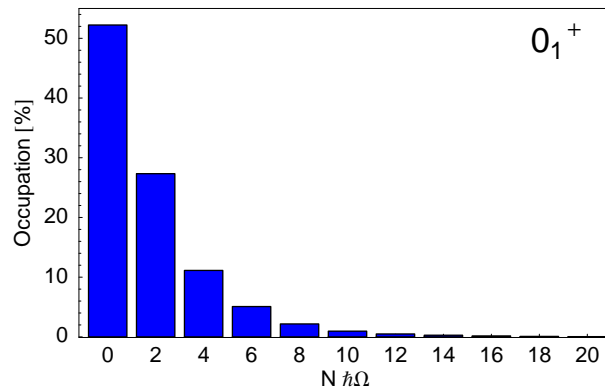
Cluster States in ^{12}C

Harmonic Oscillator $N\hbar\Omega$ Excitations

Y. Suzuki *et al*, Phys. Rev. C **54**, 2073 (1996).

$$\text{Occ}(N) = \langle \Psi | \delta \left(\sum_i (H_i^{HO} / \hbar\Omega - 3/2) - N \right) | \Psi \rangle$$

Cluster Model



Include ${}^8\text{Be}-\alpha$ continuum



How to treat the ${}^{12}\text{C}$ continuum above the $3-\alpha$ threshold ?

- In principle it should be described as a three-body continuum
- However ${}^8\text{Be}+\alpha$ configurations are lower in energy than $3-\alpha$ configurations up to pretty large hyperradii
- Approximation: consider ${}^8\text{Be}(0^+)$ and ${}^8\text{Be}(2^+)$ (and additional ${}^8\text{Be}$ pseudo states) as bound states
- Could be considered as a microscopic CDCC approach

Cluster Model: ${}^8\text{Be}$ - α Continuum

${}^8\text{Be}$ - α wave functions

alpha-cluster model calculations with continuum:

Descouvemont, Baye, Phys. Rev. **C36**, 54 (1987)

Arai, Phys. Rev. **C74**, 064311 (2006)

Vasilevsky *et al.*, Phys. Rev. **C85**, 034318 (2012)

${}^8\text{Be}$ wave functions

- α - α configurations up to 9 fm distance, project on 0^+ and 2^+ , $M = 0, 1, 2$

$$|{}^8\text{Be}_{I,K}\rangle = P_{K0}^I \sum_i \{ |{}^4\text{He}(-R_i/2\mathbf{e}_z)\rangle \otimes |{}^4\text{He}(R_i/2\mathbf{e}_z)\rangle \} c_i^I$$

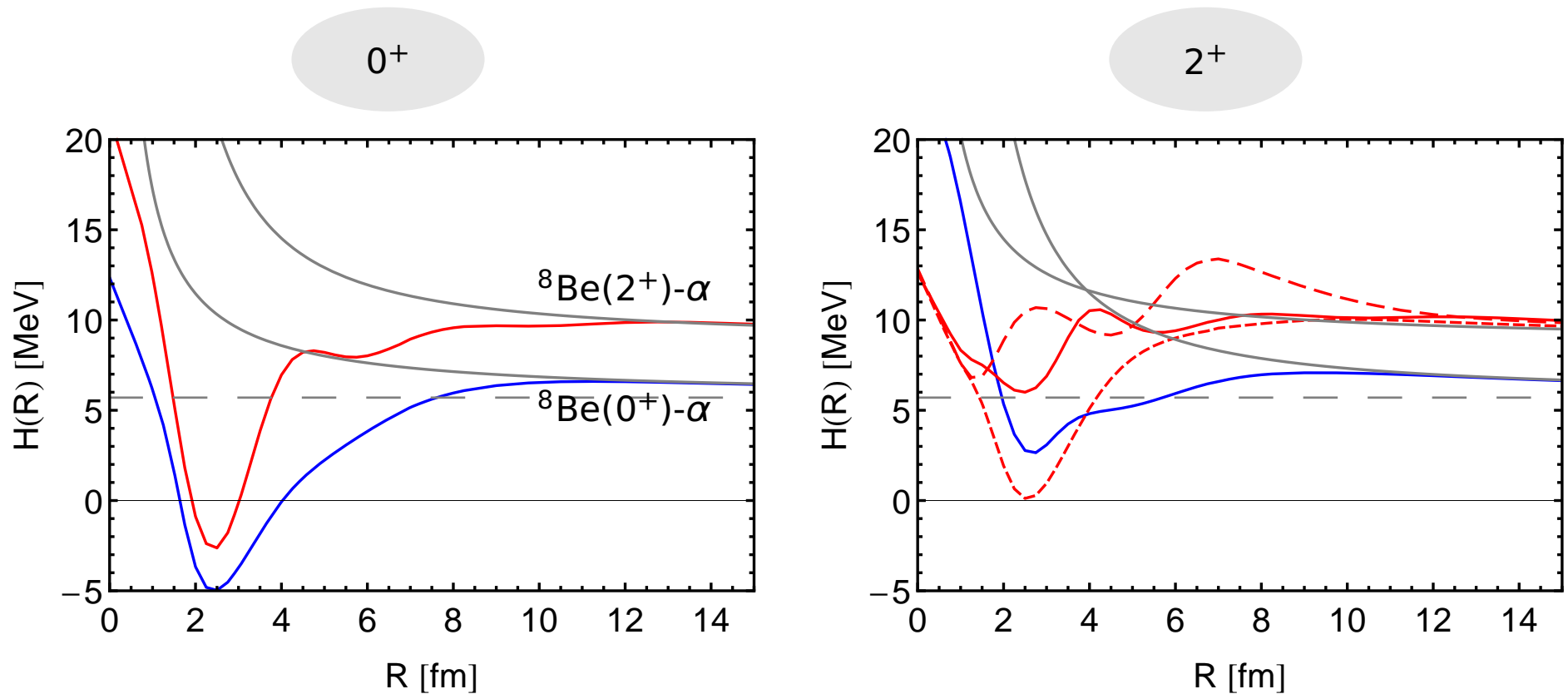
- reproduces ground state energy within 50 keV compared to full calculation

${}^{12}\text{C}$ configurations

- ${}^8\text{Be}(0^+, 2^+)$ and α at distance R
- ${}^8\text{Be}(2^+)$ can have different orientations with respect to distance vector
- ${}^8\text{Be}(0^+, 2^+) + \alpha$ configurations have to be projected on total angular momentum

$$|{}^8\text{Be}_{I,K}, {}^4\text{He}; R; JM\rangle = P_{MK}^J \{ |{}^8\text{Be}_{I,K}(-1/3R\mathbf{e}_z)\rangle \otimes |{}^4\text{He}(2/3R\mathbf{e}_z)\rangle \}$$

Cluster Model: $^8\text{Be}-\alpha$ Continuum GCM Energy Surfaces



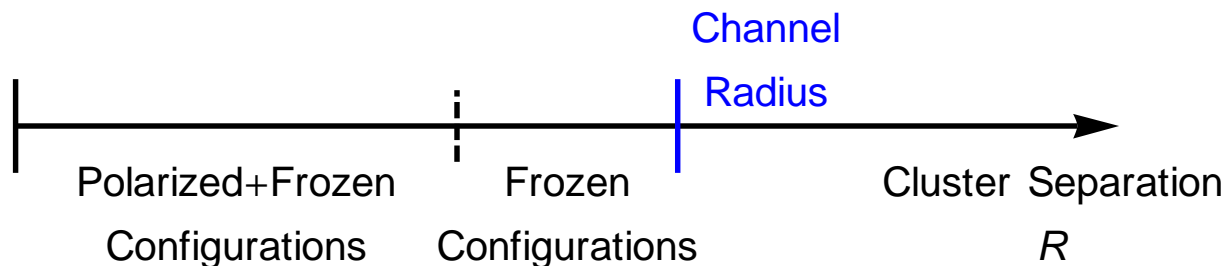
- energy surfaces contain localization energy for relative motion of ^8Be and α
- 2^+ energy surface depends strongly on orientation of ^8Be 2^+ state – $K = 2$ most attractive

Cluster Model: $^8\text{Be}-\alpha$ Continuum

Full calculation: Microscopic R -matrix Method

Model Space

- Internal region in the cluster model: 3- α configurations on a grid
- External region: $^8\text{Be}(0^+, 2^+)-\alpha$ configurations
- Channel radius has to be large: only Coulomb interaction between ^8Be and α and Coulomb coupling between different ^8Be channels should be small
- Check that results are independent from channel radius: used $a = 16.5$ fm here



Scattering Solutions

- Obtain scattering matrix using multichannel microscopic R -matrix approach
Descouvemont, Baye, Phys. Rept. 73, 036301 (2010)
- Diagonal phase shifts and inelasticity parameters: $S_{ii} = \eta_i \exp\{2i\delta_i\}$
- Eigenphases: $S = V^{-1}DV, D_{\alpha\alpha} = \exp\{2i\delta_\alpha\}$

Slater determinants and RGM wave functions

- Divide model space into internal and external region at channel radius a
- In internal region wave function is described microscopically with FMD Slater determinants
- In external region wave function is considered as a system of two point-like clusters
- (Microscopic) cluster wave function – Slater determinant

$$|Q^{ab}(\mathbf{R})\rangle = \frac{1}{\sqrt{C_{ab}}} \mathcal{A} \left\{ |Q^a(-\frac{m_b}{m_a + m_b}\mathbf{R})\rangle \otimes |Q^b(\frac{m_a}{m_a + m_b}\mathbf{R})\rangle \right\}$$

- Projection on total linear momentum decouples intrinsic motion, relative motion of clusters and total center-of-mass

$$|Q^{ab}(\mathbf{R}); \mathbf{P} = 0\rangle = \int d^3r \tilde{\Gamma}(\mathbf{r} - \mathbf{R}) |\Phi^{ab}(\mathbf{r})\rangle \otimes |\mathbf{P}_{cm} = 0\rangle$$

using RGM basis states

$$\langle \boldsymbol{\rho}, \xi_a, \xi_b | \Phi^{ab}(\mathbf{r}) \rangle = \frac{1}{\sqrt{C_{ab}}} \mathcal{A} \left\{ \delta(\boldsymbol{\rho} - \mathbf{r}) \Phi^a(\xi_a) \Phi^b(\xi_b) \right\}$$

RGM norm kernel

$$n^{ab}(\mathbf{r}, \mathbf{r}') = \langle \Phi^{ab}(\mathbf{r}) | \Phi^{ab}(\mathbf{r}') \rangle$$

Slater determinants and RGM wave functions

- Relative motion in Slater determinant described by Gaussian

$$\tilde{\Gamma}(\mathbf{r} - \mathbf{R}) = \left(\frac{\beta_{\text{rel}}}{\pi^2 a_{\text{rel}}} \right)^{3/4} \exp \left(-\frac{(\mathbf{r} - \mathbf{R})^2}{2a_{\text{rel}}} \right)$$

with

$$a_{\text{rel}} = \frac{a_a A_b + a_b A_a}{A_a A_b}, \quad \beta_{\text{rel}} = \frac{a_a a_b}{a_a A_b + a_b A_a}$$

- Overlap of full wave function with RGM cluster basis

$$\psi(\mathbf{r}) = \int d^3 r' n^{1/2}(\mathbf{r}, \mathbf{r}') \langle \Phi(\mathbf{r}') | \Psi \rangle$$

- Match asymptotics to Whittaker, outgoing Coulomb or Coulomb functions

$$\psi_b(r) = A \frac{1}{r} W_{-\eta, L+1/2}(2\kappa r), \quad \psi_{\text{Gamow}}(r) = A \frac{1}{r} O_L(\eta, \kappa r)$$

$$\psi_{\text{scatt}}(r) = \frac{1}{r} \{ I_L(\eta, \kappa r) - e^{2i\delta} O_L(\eta, \kappa r) \}$$

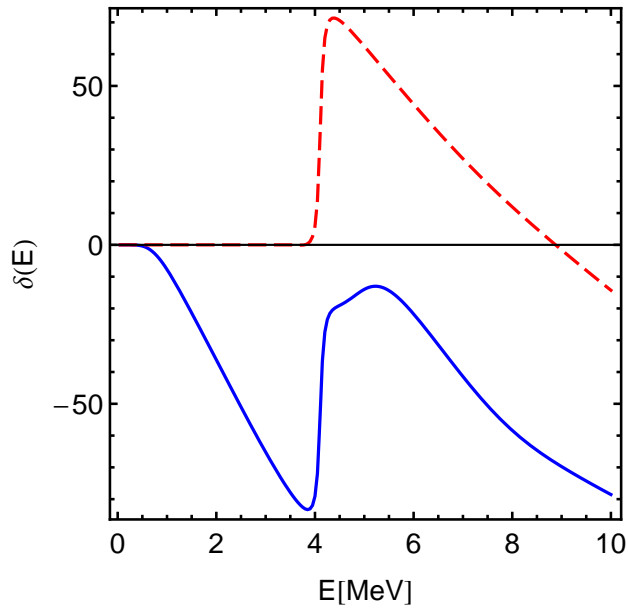
with

$$\kappa = \sqrt{-2\mu E_b}, \quad k = \sqrt{2\mu E}, \quad \eta = \mu \frac{Z_a Z_b e^2}{k}$$

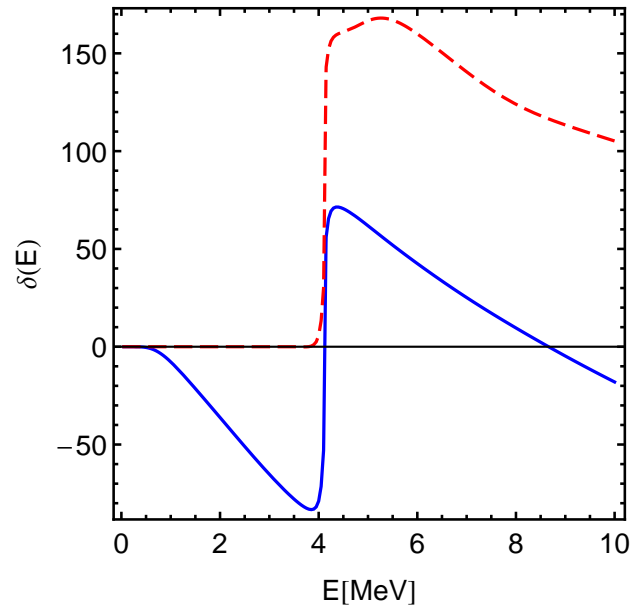
Cluster Model: $^8\text{Be}-\alpha$ Continuum

0^+ Phase shifts

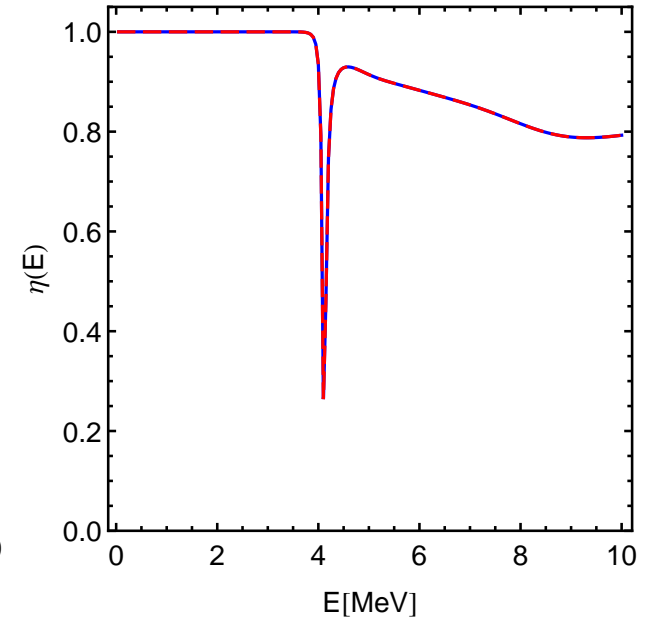
Eigenphaseshifts



Phaseshifts



Inelasticities



Gamow states

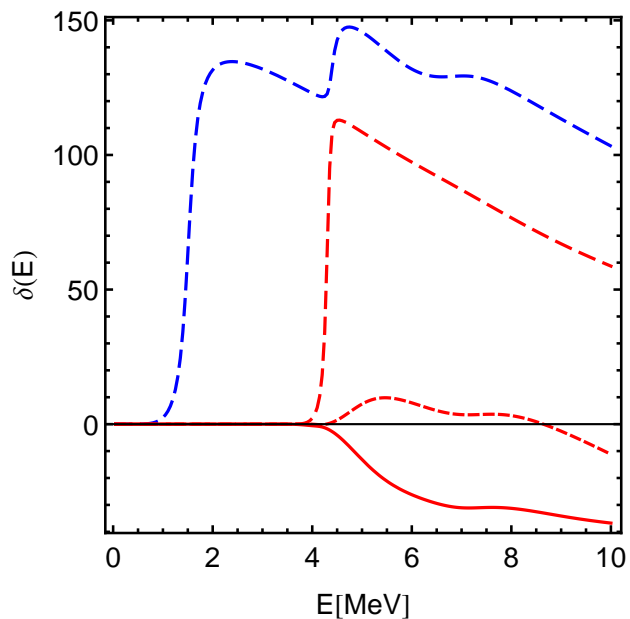
| | E [MeV] | Γ [MeV] | |
|---------|---------|----------------------|-----|
| 0_2^+ | 0.29 | $1.78 \cdot 10^{-5}$ | |
| 0_3^+ | 4.11 | 0.12 | |
| 0_4^+ | 4.76 | 1.57 | (?) |

- non-resonant background
- strong coupling between $^8\text{Be}(0^+)$ and $^8\text{Be}(2^+)$ channel at 4.1 MeV
- Hoyle state not resolved in phase shifts
- stability of broad resonance with respect to channel radius ?

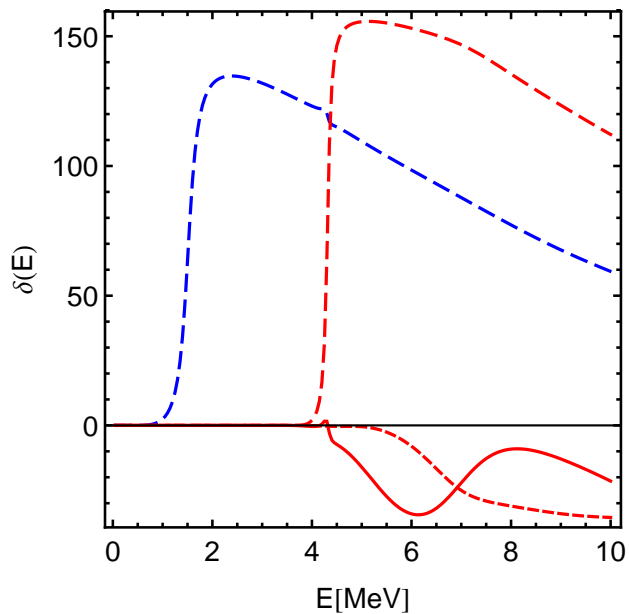
Cluster Model: ${}^8\text{Be}-\alpha$ Continuum

2^+ Phase shifts

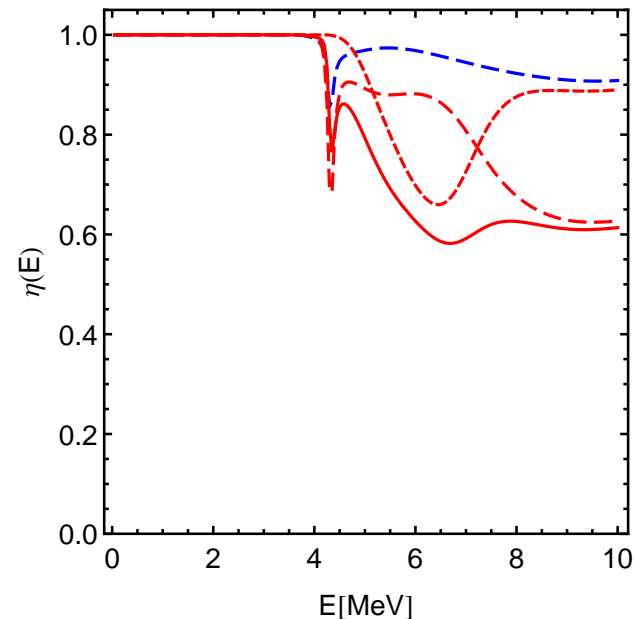
Eigenphaseshifts



Phaseshifts



Inelasticities



Gamow states

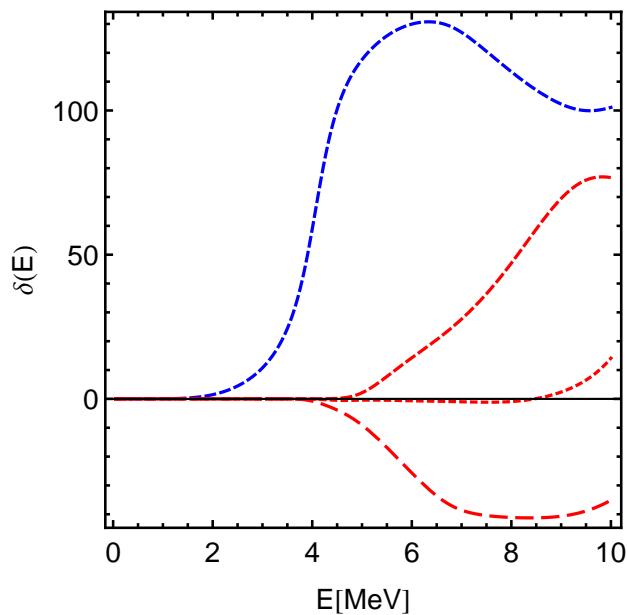
| | E [MeV] | Γ [MeV] |
|---------|---------|----------------|
| 2_2^+ | 1.51 | 0.32 |
| 2_3^+ | 4.31 | 0.14 |
| ... | | |

- non-resonant background
- strong $L = 2$ ${}^8\text{Be}(0^+)$ and ${}^8\text{Be}(2^+)$ resonances

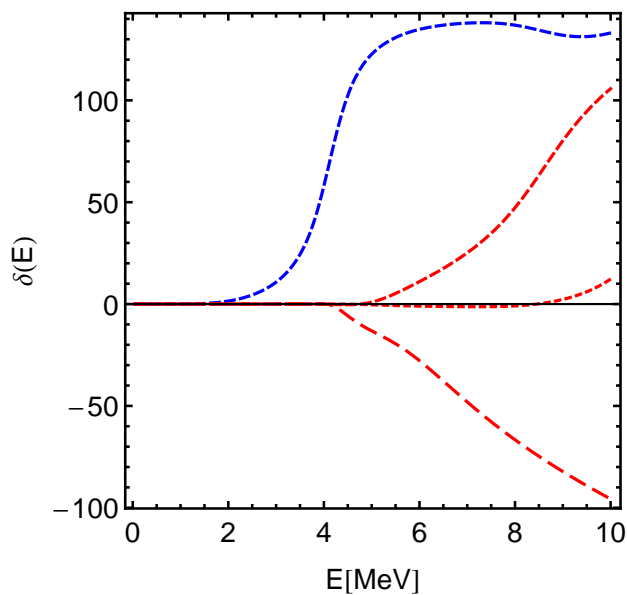
Cluster Model: $^8\text{Be}-\alpha$ Continuum

4^+ Phase shifts

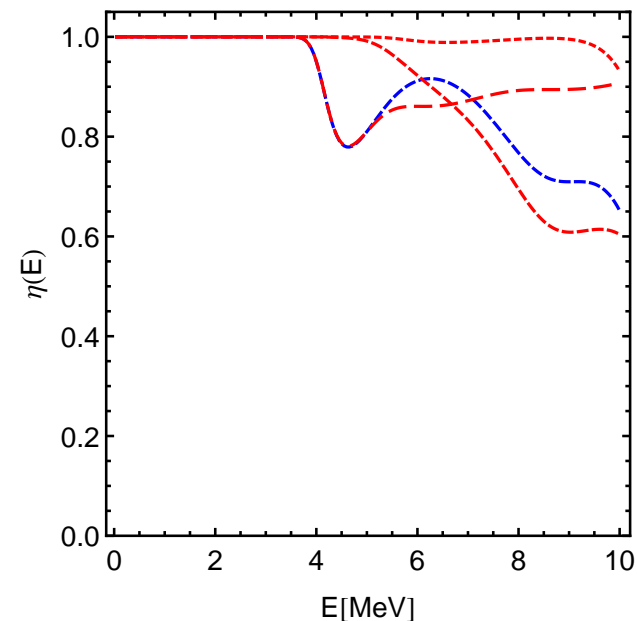
Eigenphaseshifts



Phaseshifts



Inelasticities



Gamow states

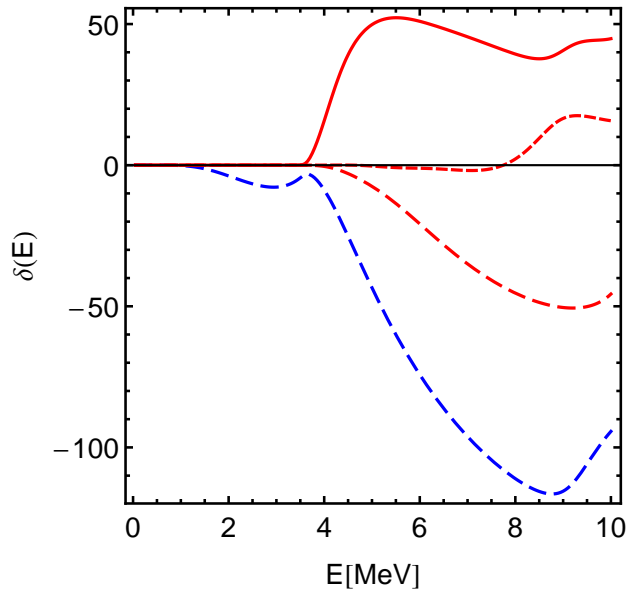
| | E [MeV] | Γ [MeV] |
|---------|---------|----------------------|
| 4_1^+ | 1.17 | $8.07 \cdot 10^{-6}$ |
| 4_2^+ | 4.06 | 0.98 |
| ... | | |

- 4_1^+ state very narrow, not resolved in phase shifts
- 4_2^+ state mostly $^8\text{Be}(0^+)$

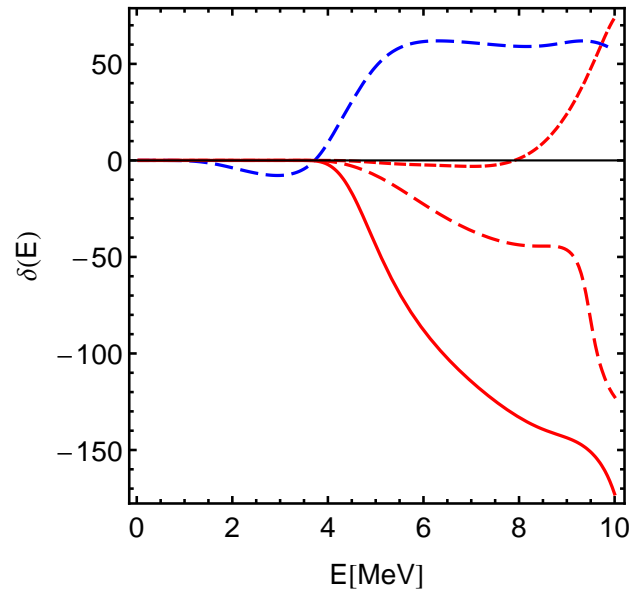
Cluster Model: $^8\text{Be}-\alpha$ Continuum

3^- Phase shifts

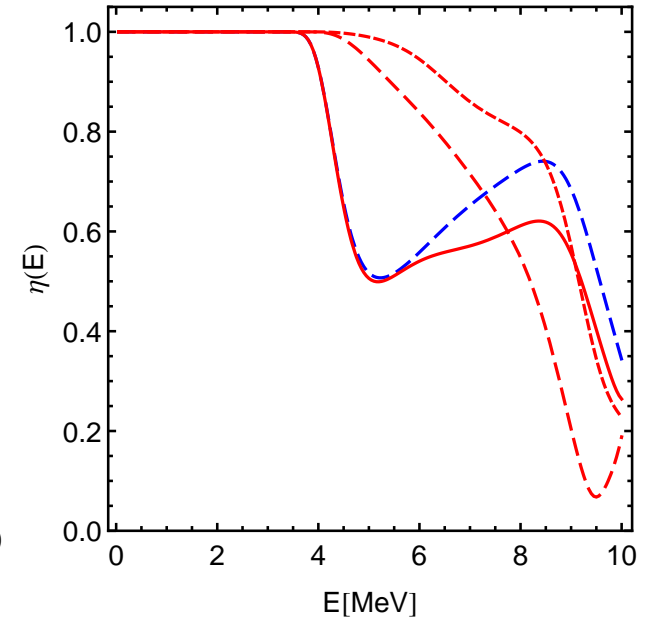
Eigenphaseshifts



Phaseshifts



Inelasticities



Gamow states

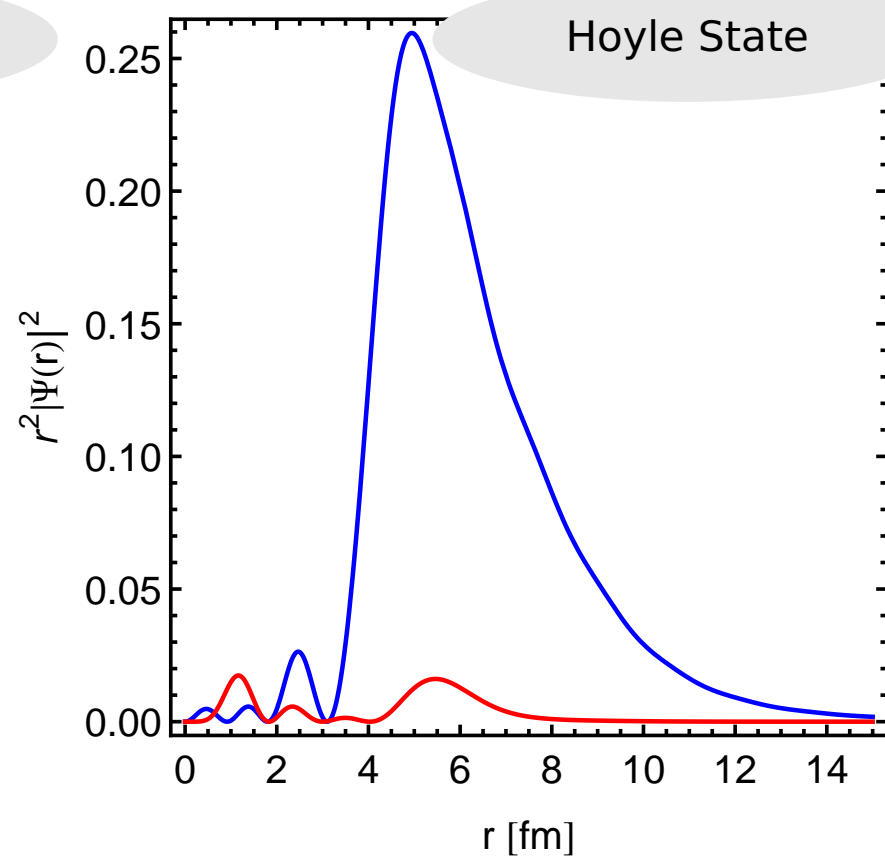
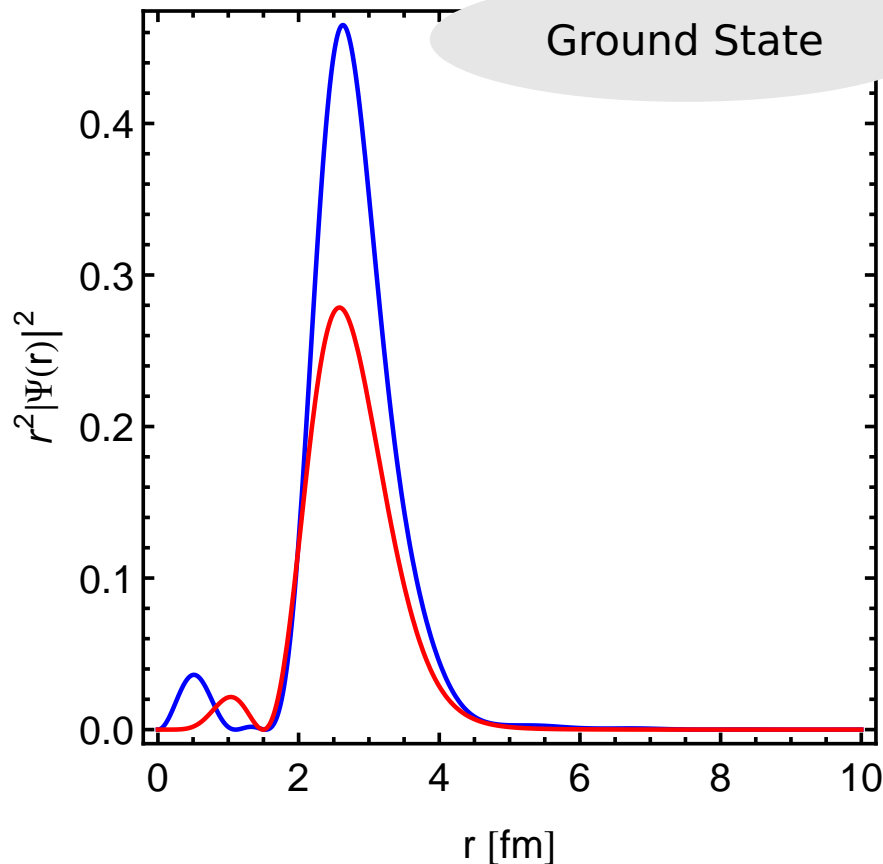
| | E [MeV] | Γ [MeV] |
|---------|---------|----------------------|
| 3^-_1 | 0.54 | $4.46 \cdot 10^{-6}$ |
| ... | | |

- 3^-_1 state very narrow, not resolved in phase shifts

Cluster Model: ${}^8\text{Be}-\alpha$ Continuum

Overlap functions

$$\psi(\mathbf{r}) = \int d^3r' n^{1/2}(\mathbf{r}, \mathbf{r}') \langle \Phi(\mathbf{r}') | \Psi \rangle$$



- Ground state overlap with ${}^8\text{Be}(0^+)+\alpha$ and ${}^8\text{Be}(2^+)+\alpha$ configurations of similar magnitude
- Hoyle state overlap dominated by ${}^8\text{Be}(0^+)+\alpha$ configurations, large spatial extension

Work in Progress: FMD calculation with $^8\text{Be}-\alpha$ Continuum



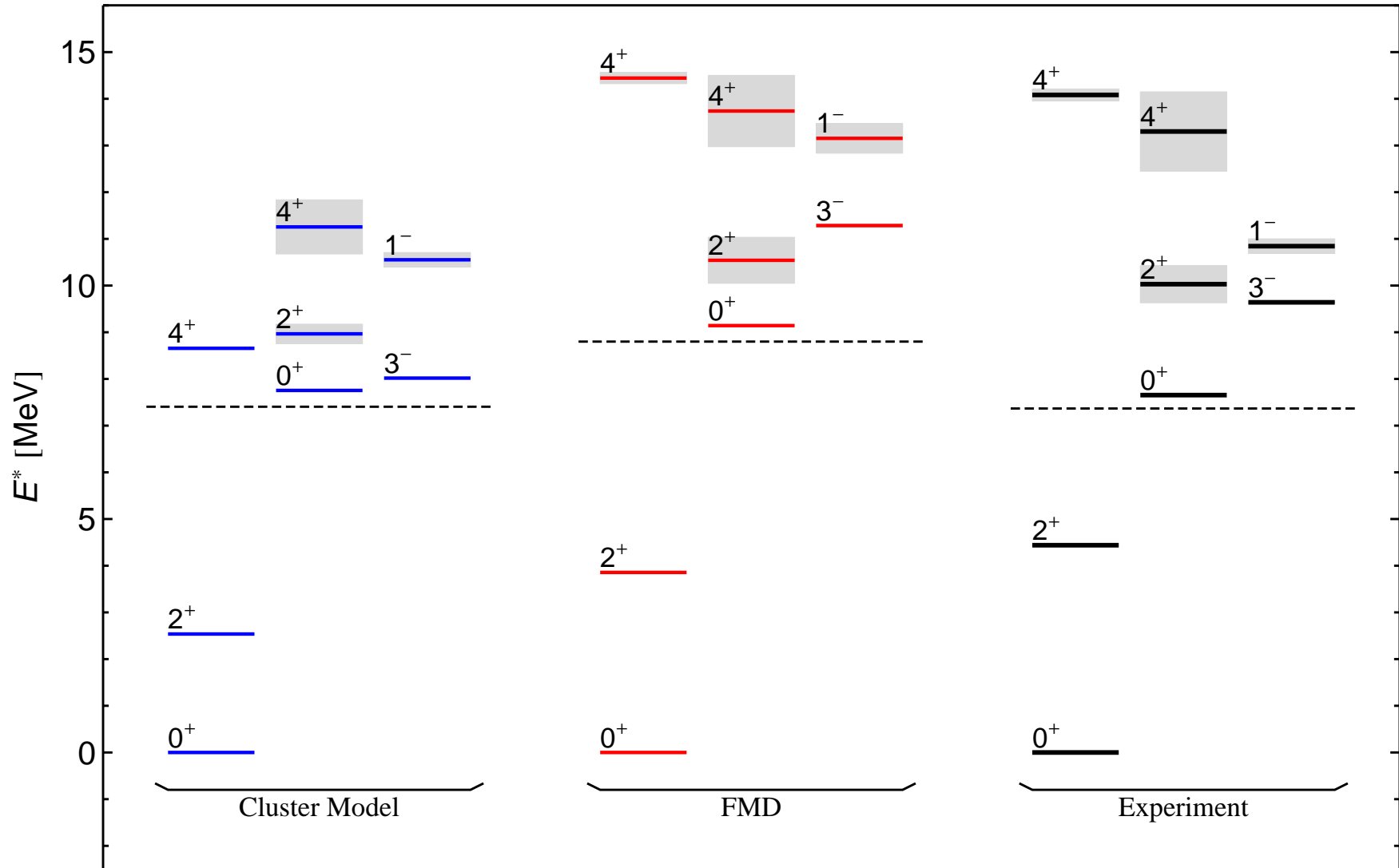
UCOM interaction

- Correlation functions from SRG $\lambda = 1.5\text{fm}^{-1}$
- Increase strength of spin-orbit force to partially account for omitted three-body forces

$^8\text{Be}-\alpha$ Continuum

- To get a reasonable description of ^8Be it is essential to include polarized configurations
- ➔ Calculate strength distributions
- ➔ Investigate non-cluster states: non-natural parity states, $T = 1$ states, M1 transitions, ^{12}B and ^{12}N β -decay into ^{12}C , ...

FMD/Cluster Model: ^8Be - α Continuum Spectra (preliminary)



- FMD: ^8Be wave functions still relatively poor

Summary

Unitary Correlation Operator Method

- Explicit description of short-range central and tensor correlations

Fermionic Molecular Dynamics

- Gaussian wave-packet basis contains HO shell model and Brink-type cluster states

Cluster States in ^{12}C

- Consistent description of ground state band and clustered states including the Hoyle state
- Test Hoyle state structure with electron scattering

The ^{12}C Continuum

- Include $^8\text{Be}(0^+, 2^+) + \alpha$ continuum in cluster model
- Hoyle state can be understood as $^8\text{Be}(0^+) + \alpha$
- First results for FMD with continuum

Thanks to my collaborators:

Hans Feldmeier (GSI), Katharine Henninger (GSI), Heiko Hergert (OSU), Wataru Horiuchi (Hokkaido), Lukas Huth (GSI), Karlheinz Langanke (GSI), Robert Roth (TUD), Yasuyuki Suzuki (Niigata), Dennis Weber (GSI)